이학박사 학위논문

Bispecific anti-mPDGFRβ/cotinine fusion protein can form antibody-drug conjugate-like complexes with cotinine-duocarmycin and exert cytotoxicity against mPDGFRβ expressing cells

이중 항체 항-mPDGFRβ/코티닌 융합 단백질은 코티닌-듀오카마이신과 항체-약물 접합체를 모사하는 형태를 이뤄 mPDGFRβ를 발현하는 세포에 독성을 발휘함

2020 년 2 월

서울대학교 대학원

의학과 협동과정 종양생물학전공

김 수 현

A thesis of the Degree of Doctor of Philosophy

이중 항체 항-mPDGFRβ/코티닌 융합 단백질은 코티닌-듀오카마이신과 항체-약물 접합체를 모사하는 형태를 이뤄 mPDGFRβ를 발현하는 세포에 독성을 발휘함

Bispecific anti-mPDGFRβ/cotinine fusion protein can form antibody-drug conjugate-like complexes with cotinine-duocarmycin and exert cytotoxicity against mPDGFRβ expressing cells

February 2020

The Department of cancer biology,

Seoul National University

College of Medicine

SOOHYUN KIM

이중 항체 항-mPDGFRβ/코티닌 융합 단백질은 코티닌-듀오카마이신과 항체-약물 접합체를 모사하는 형태를 이뤄 mPDGFRβ를 발현하는 세포에 독성을 발휘함

지도 교수 정 준 호

이 논문을 이학박사 학위논문으로 제출함

2019 년 10 월

서울대학교 대학원

협동과정 종양생물학 전공

김 수 현

김수현의 이학박사 학위논문을 인준함

2020년 1월

위 원 장 _____ (인)

부위원장 _____ (인)

위 원 _____ (인)

위 원 _____ (인)

위 원 _____ (인)

Bispecific anti-mPDGFRβ/cotinine fusion protein can form antibody-drug conjugate-like complexes with cotinine-duocarmycin and exert cytotoxicity against mPDGFRβ expressing cells

by

SOOHYUN KIM

A thesis submitted to the Department of cancer biology in partial fulfillment of the requirements for the Degree of Doctor of Philosophy in Cancer Biology at Seoul National University College of Medicine

January 2020

Approved by Thesis Committee:

Professor _____**Chairman**

Professor _____**Vice chairman**

Professor _____

Professor _____

Professor _____

Abstract

Traditionally, antibody selection for antibody-drug conjugates (ADCs) has depended on internalization of the antibody into the target cell and yet efficacy of the ADC also relies on recycling of the receptor-ADC complex, endo-lysosomal trafficking, and subsequent linker/antibody proteolysis. Here, we describe a novel ADC development platform composed of bispecific single-chain variable fragment (scFv)-kappa constant region (Cκ)-scFv fusion protein that simultaneously binds to an antigen of interest and a hapten conjugated to a cytotoxic agent. We selected cotinine as an ideal hapten due to its non-toxicity and absence from the biological system. In this study, we prepared bispecific anti-murine platelet-derived growth factor receptor beta (mPDGFRβ)/cotinine scFv-Cκ-scFv fusion protein and cotinine-duocarmycin and observed that they can form an ADC-like complex and induce cytotoxicity against mPDGFRβ expressing cells. Multiple anti-mPDGFRβ antibody candidates can be produced in this bispecific scFv-Cκ-scFv fusion protein format and tested for their ability in delivering cotinine-conjugated cytotoxic drugs, thus providing an improved approach for antibody selection in ADC development.

Keyword : Antibody-drug conjugate, Bispecific antibody, Cotinine, Duocarmycin

Student Number : 2015-22055

Contents

List of Tables

List of figures

1. Introduction

Antibody-drug conjugates (ADCs) are a class of therapeutics consisting cytotoxic drug-linked antibody that deliver cytotoxic agents to target specific antigen-positive tumor cells with minimized off-target toxicity [1, 2]. The concept of ADCs was conceptualized by Paul Ehrlich in 1906 as a "magic bullet" that targets specific antigens [3]. Although first Food and Drug Administration (FDA)-approved ADC, gemtuzumab ozogamicin (Mylotarg; Pfizer/Wyeth Pharmaceuticals), was removed from the U.S. market in 2010, three further ADCs [brentuximab vedotin (Adcetris; Seattle Genetics), ado-trastuzumab emtansine (Kadcyla; Genentech), and inotuzumab ozogamicin (Besponsa; Pfizer/Wyeth Pharmaceuticals)] were FDA-approved for the treatment of lymphoma, human epidermoid growth factor receptor-2 (HER2)-positive metastatic breast cancer, and B-cell acute lymphoblastic leukemia, respectively [4]. Moreover, gemtuzumab ozogamicin was re-approved from the FDA after a recent meta-analysis of randomized studies showed improvement in overall survival in patients with acute myeloid leukemia [5]. Currently, there are more than 65 ADCs in clinical trials [6].

Designing of ADC is a complex procedure that requires consideration of antibody, class of payload, conjugation sites, linker, tumor type, expression of antigen, and drug-to-antibody ratios (DARs) [7]. Conjugation sites for example, alters efficiency of conjugation, stability as well as affinity [8, 9, 10]. ADCs are internalized into the cell in order to release the drug payloads, and hence cytotoxic efficacy of ADC is largely dependent on the delivery efficiency of drug payloads [11]. To further complicate the situation, even when the antibodies bind to the same target on cell surface, the internalization efficiency of antibodies varies. As a result, selection of

an antibody with efficient internalization is critical for the development of ADC. There are several methods for characterization of antibody internalization. For example, use of radiolabeled antibodies [12, 13], a combination of flow cytometry and surface quenching [14, 15], confocal imaging and image analysis with high-content readers [16, 17]. A homogeneous (no-wash) high-throughput assay with antibody labeled with a pH-sensitive cyanine dye derivative, CypHer3E, was also developed [11]. Acidic environment of endocytic compartments, fluorescence CypHer3E, allows differentiation between surface bound and internalized antibodies. Nevertheless, accurate comparison of cytotoxicity using these rapidly internalizing antibodies can only be performed after production of the actual ADC as other factors such as recycling of the target antigen-ADC complex and intracellular trafficking affect efficacy of the ADC [18, 19, 20]. Consequently, significant time and effort are used to generate ADC candidates using numerous antibodies.

Platelet-derived growth factor receptor beta (PDGFRβ) is highly involved in angiogenesis and is mainly overexpressed on pericytes [21]. PDGFRβ blocking antibody was tested in a model of corneal and choroidal neovascularization as a combination therapy with an anti-VEGF DNA aptamer and was more effective in causing vessel regression at neovascular growth sites than anti-VEGF-A treatment alone, representing a potential treatment strategy for ocular angiogenic disease [22]. Neutralizing PDGFRβ antibodies also reduced choroidal neovascularization in a mouse model of age-related macular degeneration due to blocking of pericyte function [23]. The PDGFRβ specific Affibody molecule accumulated near tumor blood vessels in a model of spontaneous insulinoma, confirming the protein's potential for *in vivo* tumor targeting [24]. Recently, a radiolabeled PDGFRβ specific,

high affinity Affibody enabled tumor visualization [25], and an Affibody-photosensitive dye conjugate successfully inhibited colorectal cancer growth in a mouse xenograft model [26]. An aptamer against PDGFRβ was also developed which has a K_D of 500 pM and blocks binding of PDGF-BB with a K_D of 1.5 nM [27]. The dimerization of PDGFRβ induced by a PDGF dimer or other artificial measure was essential and sufficient to drive PDGFRβ internalization independent of PDGFRβ kinase activation [28], it is not known how the aptamer induced receptor internalization. Taken together, many PDGFRβ blocking antibody and Affibody molecules have been developed, but no efficiently internalizing anti-PDGFRβ antibody has been reported.

In this study, we report a new screening platform that ease the selection of antibody with efficient delivery of payloads into the target cells. The platform is composed of hapten-conjugated drugs and bispecific single-chain variable fragment (scFv)-human kappa constant (Cκ)-scFv fusion proteins that bind an antigen of interest (Fig. 1A). There are numerous advantages of this approach. Cotinine is a major metabolite of nicotine and is an ideal hapten for our platform due to its non-toxicity, physiological inertness and exogeneity [29]. Furthermore, the synthesis of hapten-conjugated drug is eased due to commercially available trans-4-cotinine carboxylic acid that can be chemically cross-linked to various molecules [30]. As a result, synthesis of various cotinine-drugs with different combinations of cytotoxic drugs and linkers are possible while its purity better ensured than the conventional ADCs. Because the drug does not require direct conjugation to the antibody, it would not alter affinity and stability of antibodies. Finally, formation of ADCs only requires a simple mixing of bispecific antibody and cotinine-drug conjugate.

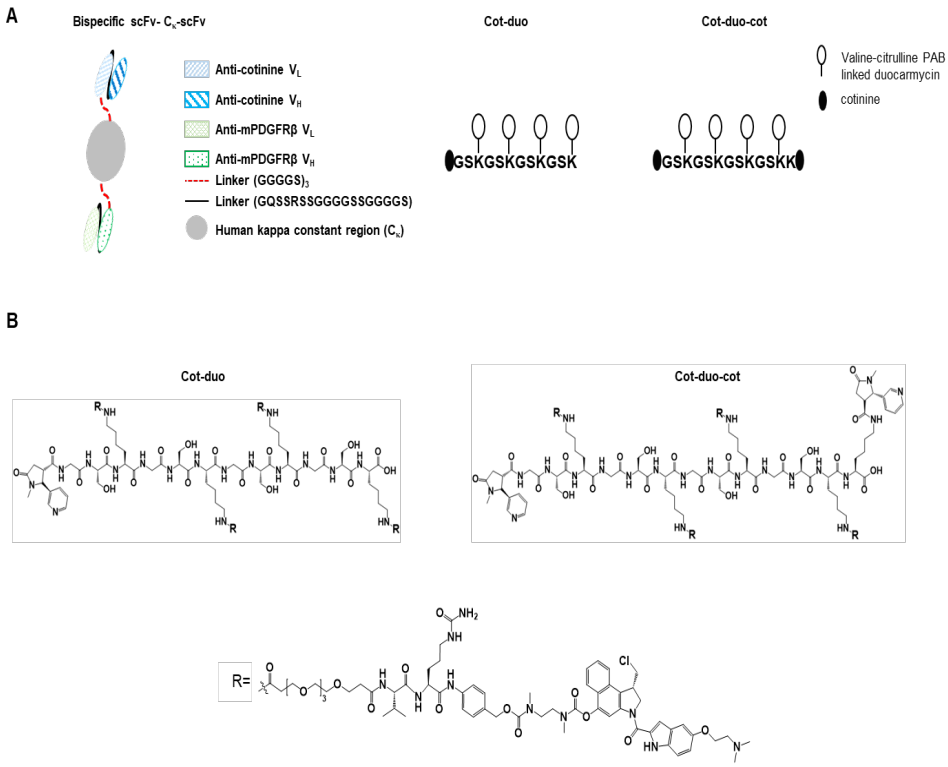

Fig. 1. Bispecific anti-mPDGFRβ/cotinine scFv-Cκ-scFv fusion protein and cotinine-conjugated duocarmycin. (A) Schematic diagrams of the fusion protein and cotinine-conjugated duocarmycin (cot-duo and cot-duo-cot). (B) Chemical structures of cot-duo and cot-duo-cot. "R" represents valine-citrulline PAB-linked dimethyl aminoethyl duocarmycin.

The feasibility of this platform was tested using an anti-mPDGFRβ/cotinine bispecific scFv-Cκ-scFv fusion protein. We constructed monovalent and bivalent cotinine-conjugated peptides cross-linked to duocarmycin, termed cotinine-duocarmycin (cot-duo) and cotinine-duocarmycin-cotinine (cot-duo-cot), respectively (Fig. 1B). The bispecific scFv-Cκ-scFv fusion proteins complexed with cotinine-duocarmycin conjugates were tested *in vitro* to select efficiently internalizing anti-mPDGFRβ antibody and the complex exhibited cytotoxicity against murine NIH3T3 cell lines expressing PDGFRβ and inhibited neovascularization *in vivo*. Our results indicate optimal antibodies and cytotoxic drug combinations for ADC can be screened out using our platform.

2. Materials and Methods

2. 1. Expression and purification of recombinant mPDGFRβ-Cκ fusion protein

Genes encoding the extracellular domain of mPDGFRβ with two *SfiI* endonuclease recognition sites were chemically synthesized (GenScript Biotech, Jiangsu, China), digested with restriction enzyme *SfiI* (New England Biolabs, Hertfordshire, UK), and were ligated into pCEP4 vector for expression as a Cκ fusion protein as described earlier [31].

The recombinant pCEP4 expression vector was transfected into human embryonic kidney (HEK)293F cells (Invitrogen, Carlsbad, CA, USA) using polyethyleneimine (Polysciences, Warrington, PA, USA) as described earlier [32]. Transfected cells were cultured in GIBCO FreeStyle 293 expression medium (Invitrogen) that contains 10,000 IU/L penicillin and 100 mg/L streptomycin (Invitrogen) [33]. The culture supernatants were collected for purification by affinity chromatography using KappaSelect resin (GE Healthcare, Buckinghamshire, UK) at day 6 post-transfection following the manufacturer's protocol.

2. 2. Cell culture

NIH3T3 cells were obtained from the Korean Cell Line Bank (Seoul, Republic of Korea) and maintained in Dulbecco's modified Eagle's medium (DMEM; Welgene, Seoul, Korea) supplemented with 10% fetal bovine serum (FBS; GIBCO, Grand Island, NY, USA) and 1% penicillin/streptomycin [30].

MOLT-4 cells were obtained from the Korean Cell Line Bank and were maintained in RPMI-1640 (Welgene, Seoul, Republic of Korea) supplemented with 10% FBS (GIBCO) and 1% penicillin/streptomycin.

2. 3. Immunization of chicken

Five white leghorn chickens were immunized and boosted three times with 5 μg of mPDGFRβ-Fc chimera (1042-PR-100; R&D Systems, Minneapolis, MN, USA). Blood samples were collected from wing veins before and during the immunizations for enzyme immunoassays and flow cytometry analysis for evaluation of the chicken's immunization status.

2. 4. Generation of combinatorial scFv-displayed phage library and bio-panning

Chickens were sacrificed a week after the third booster, and their bursae of Fabricius, bone marrows and spleen were harvested for total RNA isolation using TRI Reagent (Invitrogen). cDNA was synthesized using Superscript® III First-Strand Synthesis system (Invitrogen) for generation of a scFv-displayed phage library as described earlier [34]. The phage libraries were subjected to five rounds of bio-panning against mPDGFRβ-Cκ-conjugated magnetic beads [31]. The scFv clones were selected randomly from the output titer plate of the last round and subjected to a phage enzyme immunoassay against mPDGFRβ-Cκ-coated microtiter plates (3690; Corning Life Sciences, Corning, NY, USA) [35]. Clones reactive (A405 > 1.5) against mPDGFRβ-Cκ fusion protein were sent for sequencing using OmpSeq

primers [36] by Macrogen (Seoul, Korea).

2. 5. Expression and purification of bispecific scFv-Cκ-scFv fusion protein

pCEP4 expression vector encoding bispecific scFv-Cκ-scFv fusion protein was constructed. Briefly, anti-mPDGFRβ scFv, and anti-cotinine scFv genes were cloned into the expression vector after being digested with *Sfi1*, *AgeI*, and *NotI* (New England Biolabs), respectively. Trastuzumab scFv was cloned into the vector as a control for anti-mPDGFRβ scFv. The C-terminal cysteine residue of Cκ was excluded to abolish the dimerization of scFv- Cκ-scFv fusion proteins through disulfide bond formation. The constructs were then transfected into HEK293F cells, and scFv-Cκ-scFv fusion proteins were purified using KappaSelect resin as described above.

For the confirmation of protein purity, SDS-polyacrylamide gel electrophoresis was performed using NuPage 4-12% Bis-Tris gels (Invitrogen) following the manufacturer's protocol. Briefly, 1 μg of protein dissolved in LDS sample buffer with or without reducing agents was boiled for 10 min at 95°C. The samples were then electrophoresed, and the gel was incubated with Ezway Protein-Blue II staining solution (Komabiotech, Seoul, Korea) for the visualization of protein bands.

2. 6. Size-exclusion chromatography (SEC)

Anti-mPDGFRβ/cotinine bispecific scFv-Cκ-scFv fusion proteins complexed with cot-duo or cot-duo-cot were analyzed using SEC-high performance liquid

chromatography (HPLC) by Y-biologics (Daejon, Korea). Dionex Ultimate 3000 (Thermo Fisher Scientific Inc., MA, USA) equipped with a Sepax SRT-C SEC-300 column (7.8 x 300 mm) that was packed with 5 μm particles of 300 Å pore size was used. The mobile phase contained phosphate-buffered saline (PBS). Samples (1 mg/mL) in twenty microliters were injected and eluted isocratically at a flow rate of 1 mL/min for 15 min. The column effluent was monitored by an ultraviolet detector at 254 nm and displayed as mAU.

2. 7. Enzyme immunoassays

Microtiter plates were coated overnight at 4°C with 100 ng of mPDGFRβ-Fc chimera or anti-TNFα receptor extracellular domain-human Fc fusion protein (Etanercept) in coating buffer (0.1 M sodium bicarbonate, pH 8.6). Wells were blocked with 150 μL of 3% (w/v) bovine serum albumin (BSA) in PBS for 1 h at 37°C. Various dilutions of chicken sera (1:500 to 1:62,500) diluted in 3% BSA/PBS were added to the wells. After incubating the sera for 2 h at 37°C, plates were washed with 0.05% (v/v) Tween 20 in PBS (PBST) three times followed by incubation with horseradish peroxidase (HRP)-conjugated anti-chicken IgY antibodies (Millipore, Billerica, MA, USA) for 1 h at 37°C. Plates were washed again with 0.05% PBST followed by measurement using 2,2'-azino-bis-3-ethylbenzothiazoline-6-sulfonic acid solutions (Pierce, Rockford, IL, USA). Absorbance was measured at 405 nm with a Multiscan Ascent microplate reader (Labsystems, Helsinki, Finland).

Microtiter plates were coated overnight at 4°C with 100 ng of mPDGFRβ-Fc chimera or anti-TNFα receptor extracellular domain-human Fc fusion protein in coating buffer, and wells were blocked with 150 μL of 3% BSA/PBS for 1 h at 37°C. Diluted

bispecific scFv-Cκ-scFv fusion proteins (0.06 nM to 1 μM) in 3% BSA/PBS were added to the wells and incubated for 2 h at 37°C. The plates were washed with PBST three times followed by incubation with HRP-conjugated anti-human Cκ antibodies (Millipore) for 1 h at 37°C. The Plates were washed again with 0.05% PBST followed by measurement using 3,3′ ,5,5′ -tetramethyl benzidine substrate solution (TMB) (GenDEPOT, Barker, TX, USA). Absorbance was measured at 650 nm with a Multiscan Ascent microplate reader (Labsystems).

Reactivity of bispecific scFv-Cκ-scFv fusion protein to cotinine was assessed. The microtiter plates were coated overnight at 4°C with 100 ng of cotinine-conjugated BSA (cotinine-BSA) as described earlier [37]. Wells were blocked using 3% BSA/PBS followed by incubation with bispecific scFv-Cκ-scFv fusion proteins (100 nM) for 2 h at 37°C. After washing with 0.05% PBST as described above, HRP-conjugated anti-human Cκ antibody (1:4,000) (Millipore) was added for 1 h at 37°C. The amount of antibody bound to the plate was determined by adding TMB substrate solution (GenDEPOT). To confirm simultaneous binding, mPDGFRβ-Fc chimera (100 nM) was incubated in the place of HRP-conjugated anti-human Cκ antibodies followed by incubation of HRP-conjugated anti-human Fc antibodies (ThermoFisher Scientific, Waltham, MA, USA). Subsequently, TMB substrate solution was added and absorbance was measured at 650 nm with a Multiscan Ascent microplate reader (Labsystems).

For the evaluation of competitive binding between bispecific scFv-Cκ-scFv fusion protein and mPDGF-BB, microtiter plates were coated overnight at 4°C with 100 ng of mPDGFRβ-Fc chimera and blocked as described above. Various concentrations of bispecific scFv-Cκ-scFv fusion proteins (0.06 nM to 1 μM) with or without

mPDGF-BB (100 nM) were added to each well and incubated for 2 h at 37°C. Washing, incubation, and detection were performed as in the immunoassays above.

2. 8. Flow cytometry

NIH3T3 cells were incubated with 1:100 diluted chicken sera in flow cytometry buffer (1% [w/v] BSA in PBS containing 0.05% [w/v] sodium azide) at 4°C for 1 h and washed with flow cytometry buffer four times. Cells were then probed with Alexa Fluor 488-conjugated anti-chicken IgY antibodies (703-545-155, Jackson Immunoresearch, West Grove, PA, USA) in flow cytometry buffer. After washing, samples were sorted using a FACS Canto II instrument (BD Biosciences, San Jose, CA, USA). Ten thousand cells were detected per measurement, and results were analyzed using FlowJo (Tree Star, Ashland, OR, USA).

mPDGF-BB (315-18; Peprotech, Rocky Hill, NJ, USA) was biotinylated using biotin-xx microscale protein labeling kit (Invitrogen) following the manufacturer's protocol. NIH3T3 cells were incubated with bispecific scFv-Cκ-scFv fusion proteins (100 nM) with or without mPDGF-BB-biotin (100 nM) in flow cytometry buffer at 4°C for 1 h. Cells were washed with flow cytometry buffer four times and probed with allophycocyanin (APC)-conjugated anti-human Cκ antibody (clone TB28-2; BD Biosciences, San Jose, CA, USA) or streptavidin-phycoerythrin (PE) (12-4317-87; eBioscience, ThermoFisher) in flow cytometry buffer. After washing, samples were sorted using a FACS Canto II instrument (BD Biosciences, San Jose, CA, USA). Ten thousand cells were detected per measurement, and results were analyzed using FlowJo (Tree Star, Ashland, OR, USA).

MOLT-4 cells were incubated with bispecific scFv-Cκ-scFv fusion proteins (100 nM)

in flow cytometry buffer at 4°C for 1 h. Washing and detection using APC-conjugated anti-human Cκ antibody were performed as in the flow cytometry assay above.

2. 9. Confocal microscopy for visualizing internalization of bispecific scFv-Cκ-scFv fusion proteins

NIH3T3 cells were incubated with DMEM containing 10% (v/v) FBS and bispecific scFv-Cκ-scFv fusion proteins (10 μg/mL) for 30 min at 37°C for internalization. Cells were washed with cold PBS three times and incubated with acidic buffer (0.2 M acetic acid, 0.5 M NaCl) for 5 min at room temperature to remove cell surface bound antibodies. Cells were then washed with cold PBS twice, fixed in 4% paraformaldehyde (Electron Microscopy Sciences, Hatfield, PA, USA) in PBS for 10 min, and immunofluorescent stained as described earlier [38] with some modifications. Briefly, cells were incubated with PBS containing 5% horse serum (GIBCO) and 0.1% Triton X-100 for 30 min to block binding of non-specific antibody and then with 2 μg/mL FITC-conjugated anti-human Cκ antibody (TB28-2, BD Biosciences) for 30 min at room temperature. To image early endosomes, cells were washed with PBS three times, exposed to PBS containing 5% horse serum and 0.1% Triton X-100 for 30 min, and incubated for 30 min with 1:200 anti-Rab5 antibody (C8B1, Cell Signaling Technology, Danvers, MA, USA) in the same solution before detection of immune complexes with Alexa Fluor 546-conjugated goat anti-rabbit IgG (A-11035, Invitrogen). Cells were stained with 0.2 μg/mL DAPI to detect DNA. Confocal images were acquired with a Zeiss LSM 880 microscope, and images were processed with Zen software (Carl Zeiss, Thornwood, NY, USA).

2. 10. Synthesis of cotinine-duocarmycin conjugates

The trans-4-cotinine carbonyl-GSKGSKGSKGSK peptide was chemically synthesized via Fmoc solid phase peptide synthesis (SPPS) using ASP48S auto peptide synthesizer by peptron, Inc. (Daejon, Korea). Trans-4-cotinine carboxylic acid (Sigma-Aldrich, St Louis, MO, USA) was attached to the N-terminus of peptide using basic Fmoc-amino acid coupling method. When the synthesis was completed, crude peptide was cleaved from the resin using a mixture of TFA/EDT/thioanisole/TIS/DW (90/2.5/2.5/2,5/2.5 volume) for 2 h. The solution was precipitated with cold ether and centrifuged to make a pellet. The pellet was collected and air dried. The crude product was then purified by reverse phase HPLC using ACE 10 C18-300 reverse phase column (250 mm x 21.2 mm, 10 μM). Elution was carried out with a water-acetonitrile linear gradient (10~75% (v/v) of acetonitrile) containing 0.1% (v/v) trifluoroacetic acid (Alfa Aesar, Warm Hill, MA, USA). Purified peptide (Cot-(GSK)4 peptide) was collected and lyophilized.

Valine-citrulline p-aminobenzyloxycarbonyl (PAB)-linked dimethylaminoethyl duocarmycin was used for conjugation to free amino groups on four lysines on the monovalent cotinine-GSKGSKGSKGSK peptide by Levena Biopharma (San Diego, CA, USA). The Cot-(GSK)4 peptide (3.5 mg, 2 μmol) was dissolved in acetonitrile/water (6/4, v/v, 1 mL). The NHS ester of PEG3-valine-citrulline PAB-linked dimethylaminoethyl duocarmycin was added, followed by 9 μL of saturated aqueous NaHCO3 solution. The reaction mixture was stirred at room temperature for 4 h and purified directly by reverse phase HPLC using Phenomenex Gemini® C18-100Å column (100 mm x 2 mm x 5 μM). The conjugated complex (cotinine-

[GSK(duocarmycin)]4, DAR4) was termed “cot-duo.” Bivalent cotinine cross-linked GSKGSKGSKGSKK peptide was also synthesized for conjugation to duocarmycin as described previously [39]. Briefly, two trans-4-cotinine carboxylic acid molecules were attached to a free amino group on the N-terminus of GSKGSKGSKGSKK and to the epsilon amino group of a C-terminal lysine using basic Fmoc-amino acid coupling method by Peptron, Inc. Four PAB-linked duocarmycin molecules were then conjugated to the bivalent cotinine cross-linked GSKGSKGSKGSKK peptide by Levena Biopharma, forming cotinine-[GSK(duocarmycin)]4K-cotinine (DAR2), abbreviated as “cot-duo-cot.”

2. 11. Complex formation of bispecific scFv-Cκ-scFv fusion proteins with cotinine conjugated duocarmycin

Anti-mPDGFRβ/cotinine scFv-Cκ-scFv fusion proteins were mixed with cot-duo or cot-duo-cot. The fusion proteins (2 μM) were combined at a molar ratio of 1:1 and 2:1 to cot-duo (2 μM) and cot-duo-cot (1 μM) in dimethyl sulfoxide (DMSO), respectively. After the complex formation for 30 min at room temperature, the complexes were 5-fold serially diluted (25.6 pM to 2 μM) in DMEM supplemented with 10% FBS and 1% penicillin/streptomycin. The complex was used for cytotoxicity test.

To check the complex formation, anti-mPDGFRβ/cotinine scFv-Cκ-scFv fusion proteins in PBS (15 μM) were combined at a molar ratio of 1:1 and 2:1 to cot-duo (15 μM) and cot-duo-cot (7.5 μM), respectively. After incubation for 30 min at room temperature, the complexes were then analyzed using SEC-HPLC.

2. 12. Cell cytotoxicity tests

NIH3T3 cells in 50 μL of DMEM supplemented with 10% FBS and 1% penicillin/ streptomycin were seeded in 96-well plates (CLS3595, Corning) and incubated overnight at 37°C in a humidified atmosphere with 5% CO2. Anti-mPDGFRβ/cotinine scFv-Cκ-scFv fusion proteins (25.6 pM to 2 μM) complexed with cot-duo or cot-duo-cot in 50 μL of DMEM media were then added to the cells in 50 μL of fresh media (12.8 pM to 1 μM) and incubated for 72 h at 37°C in a humidified atmosphere with 5% CO2. To test the effect of mPDGF-BB on the cytotoxicity of the bispecific scFv-Cκ-scFv fusion protein complexed cotinine-duocarmycin conjugates, mPDGF-BB (2 nM) was added to 50 μL of bispecific scFv-Cκ-scFv fusion protein complexed cotinine-duocarmycin conjugates. The complexes were then added to the cells in 50 μL of fresh media (1 nM). Bispecific anti-HER2/cotinine scFv-Cκ-scFv fusion protein was used as a control. After the cells were incubated for 72 h, 100 μL of Cell Titer-Glo reagents (Promega Corp., Madison, WI, USA) were added to each well, and luminescence was measured using a luminometer (PerkinElmer, Waltham, MA, USA) following the manufacturer's instructions. The experiments were conducted in triplicate. Relative cell viability was calculated by the following formula: [% viability = (the luminescent signal of the test well – the luminescent signal of the background well) / (the luminescent signal of control well – the luminescent signal of background well) × 100]. Wells containing fresh medium only were used for background measurement.

2. 13. Statistical analysis

Cytotoxicity of bispecific scFv-Cκ-scFv fusion protein was defined as IC50 (half

maximal inhibitory concentration), and statistical significance was calculated using unpaired Student's t-tests or a one-way analysis of variance. Tukey's post hoc multiple comparison test was used for further identification of significant differences between the bispecific scFv-Cκ-scFv fusion proteins. A p-value of less than 0.05 was considered statistically significant. All analyses were performed using Prism v5.0 (GraphPad Software, Inc., San Diego, CA, USA).

2. 14. Laser-induced choroidal neovascularization (CNV) mouse model

After anesthetizing mice, customized laser indirect ophthalmoscope system (ILOODA) was used to induce the rupture of Bruch's membrane (810 nm wavelength, spot size 300 um, 400 mW power and 50 ms exposure time). Four days later, bispecific scFv-Cκ-scFv, cot-duo and bispecific scFv-Cκ-scFv complexed with cot-duo (10 nM, 1 uL) were intravitreally administered. For the evaluation of the effects of the bispecific scFv-Cκ-scFv fusion protein complexed with cot-duo, RPE-choroid-scleral complexes were isolated from the enucleated eyes at seven days post laser photocoagulation. RPE-choroid-scleral complexes were immunostained with isolectin B4-594 to measure the amount of choroidal neovascularization (CNV). Quantitative analysis of the CNV area was performed using the ImageJ program (NIH).

3. Result

3. 1. Anti-mPDGFRβ antibody was selected from combinatorial scFv-displayed phage libraries generated from immunized chickens

Chickens were immunized and boosted three times with mPDGFRβ-Fc chimera. Total RNA was prepared from bone marrow, spleen and bursa of Fabricius, and was subjected to cDNA synthesis. Using the cDNA, four chicken combinatorial scFv-displayed phage libraries were generated with complexities of 7.5×10^8, 6.9×10^8, 2.1×10^9, and 2.2×10^9, respectively, and five rounds of bio-panning were performed on immobilized mPDGFRβ-Cκ fusion protein. From the output titer plates of the last round, clones were randomly selected for rescue by infection of helper phage. The reactivity of the rescued clones was tested in phage enzyme immunoassay. After sequencing, nine antibody clones were identified (Fig. 2A). Based on their expression levels and binding activities, four clones were selected for further study.

A

Clone	HCDR3 sequences
PRb-CC01	GGGSIDA
PRb-CN01	GVGSWAHGGRIDA
PRb-CC02	GYAGTIDA
PRb-CC03	SSYIDT
PRb-C11	GGAAIDA
PRb-C12	GSIPAFIDA
PRb-C13	CDGYNCGYSAAWIDA
PRb-C14	GSYGGIWGGDIDA
PRb-C15	HTGIVGTYCIDA

B

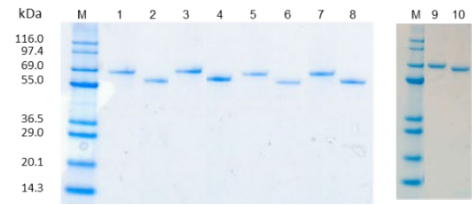

Fig. 2. Generation and characterization of bispecific scFv-Cκ-scFv fusion proteins. (A) HCDR3 amino acid sequences of anti-mPDGFRβ scFv clones. (B) Bispecific scFv-Cκ-scFv fusion proteins were subjected to SDS-polyacrylamide gel electrophoresis and staining for visualization of protein bands. Lane 1, reduced PRb-CC03/cotinine; Lane 2, non-reduced PRb-CC03/cotinine; Lane 3, reduced PRb-CC01/cotinine; Lane 4, non-reduced PRb-CC01/cotinine; Lane 5, reduced PRb-CN01/cotinine; Lane 6, non-reduced PRb-CN01/cotinine; Lane 7, reduced PRb-CC02/cotinine; Lane 8, non-reduced PRb-CC02/cotinine; Lane 9, reduced anti-HER2/cotinine (control); Lane 10, non-reduced anti-HER2/cotinine (control). M, molecular weight marker.

3. 2. Bispecific scFv-Cκ-scFv fusion proteins are overexpressed, purified and complexed with cot-duo and cot-duo-cot

An expression vector encoding anti-mPDGFRβ/cotinine scFv-Cκ-scFv fusion proteins was constructed and transfected into HEK293F cells. Bispecific scFv-Cκ-scFv fusion proteins were purified from culture supernatants through affinity column chromatography and subjected to SDS-polyacrylamide gel electrophoresis (Fig. 2B). After the gel was stained, proteins with 67 kDa or 60 kDa molecular weight were observed in lanes loaded with samples in reducing and non-reducing conditions, respectively. The computed molecular weight of the fusion proteins was 66.77 kDa. No multimeric band was observed in non-reducing samples as well as reducing samples. The non-reduced proteins migrated faster than the reduced proteins possibly due to the compactness of the native form of the protein which may offer less resistance to migration through the gel.

In SEC-HPLC analysis (Fig. 3), monomeric and trimeric form of scFv-Cκ-scFv fusion proteins were monitored in PRb-CC01, PRb-CC02 and PRb-CC03 scFv-Cκ-scFv fusion protein samples, but not in PRb-CN01 sample. When cot-duo was added to form complex with scFv-C κ -scFv fusion protein, the PRb-CC01, PRb-CC02 and PRb-CC03, significant amount of high molecular weight species (HMWS) was observed. But in case of PRb-CN01, little amount of HMWS was detected. Cot-duo-cot did not induce the formation of HMWS in all four clones.

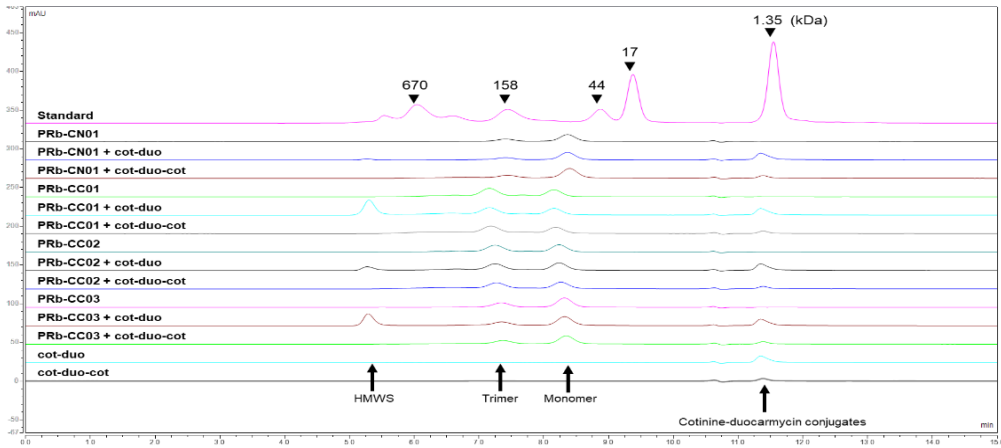

Fig. 3. Size exclusion chromatography (SEC) analysis of bispecific anti-mPDGFRβ/cotinine scFv-Cκ-scFv fusion proteins. Anti-mPDGFRβ/cotinine scFv-Cκ-scFv fusion proteins, cot-duo, cot-duo-cot and corresponding antibody conjugates were subjected to SEC-high performance liquid chromatography (HPLC) using Dionex Ultimate 3000 equipped with a Sepax SRT-C SEC-300 column. The mobile phase contained PBS. Flow rate was 1 mL/min for 15 min. Ultraviolet detection was set at 254 nm and the results were displayed as mAU. HMWS indicate high molecular weight species.

3. 3. An anti-mPDGFRβ/cotinine scFv-Cκ-scFv fusion protein simultaneously binds mPDGFRβ and cotinine in the presence of mPDGF-BB.

Enzyme immunoassays were performed to test the reactivity of the bispecific scFv-Cκ-scFv fusion proteins against mPDGFRβ and cotinine. All four cloned fusion proteins reacted to wells coated with mPDGFRβ-Fc chimera protein in a dose-dependent manner (Fig. 4A), while we observed no reactivity against negative control-human Fc protein (Fig. 4B).

All anti-mPDGFRβ/cotinine scFv-Cκ-scFv fusion proteins and control bispecific anti-HER2/cotinine scFv-Cκ-scFv fusion proteins, but not control bispecific anti-HER2/HER2 scFv-Cκ-scFv fusion protein reacted to wells coated with cotinine-BSA (Fig. 4C). To test simultaneous binding of anti-mPDGFRβ/cotinine scFv-Cκ-scFv fusion proteins to cotinine and mPDGFRβ, microtiter wells were coated with cotinine-BSA and sequentially incubated with bispecific scFv-Cκ-scFv fusion proteins, mPDGFRβ-Fc chimera proteins, and HRP-conjugated anti-human Fc antibodies with intermittent washing. Four bispecific scFv-Cκ-scFv fusion proteins (PRb-CC01, PRb-CN01, PRb-CC02, and PRb-CC03) simultaneously bound to mPDGFRβ and cotinine, while the other control bispecific fusion proteins did not (Fig. 4D).

A

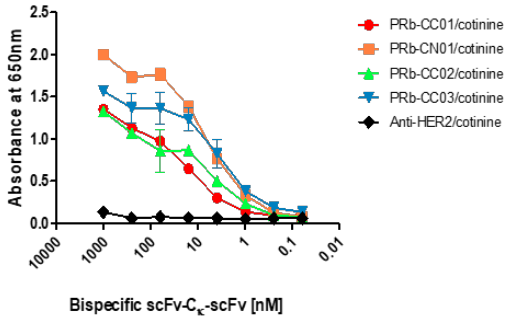
Absorbance at 650nm
2.5
2.0
1.5
1.0
0.5
0.0
10000
1000
100
10
1
0.1
0.01
Bispecific scFv-Cκ-scFv [nM]
PRb-CC01/cotinine
PRb-CN01/cotinine
PRb-CC02/cotinine
PRb-CC03/cotinine
Anti-HER2/cotinine

B

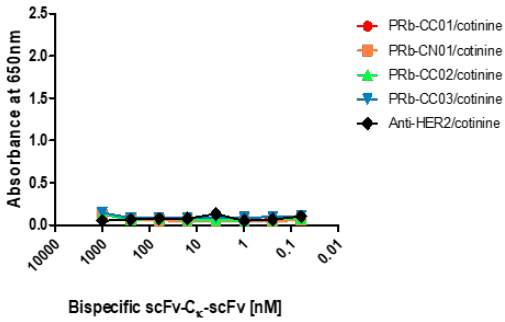
Absorbance at 650nm
2.5
2.0
1.5
1.0
0.5
0.0
10000
1000
100
10
1
0.1
0.01
Bispecific scFv-Cκ-scFv [nM]
PRb-CC01/cotinine
PRb-CN01/cotinine
PRb-CC02/cotinine
PRb-CC03/cotinine
Anti-HER2/cotinine

C

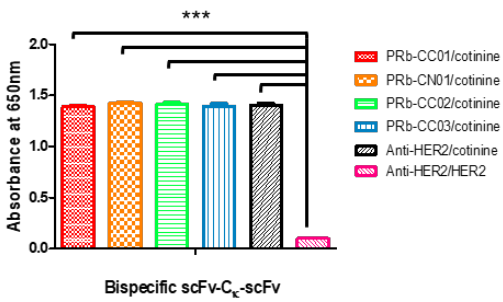
***
Absorbance at 650nm
2.0
1.5
1.0
0.5
0.0
Bispecific scFv-Cκ-scFv
PRb-CC01/cotinine
PRb-CN01/cotinine
PRb-CC02/cotinine
PRb-CC03/cotinine
Anti-HER2/cotinine
Anti-HER2/HER2

D

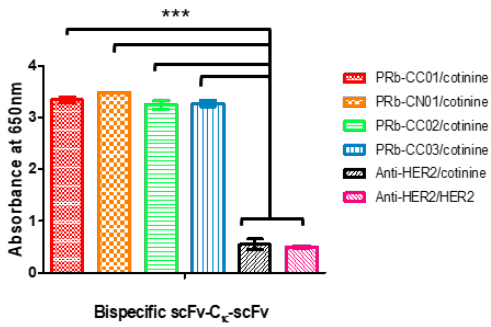
***
Absorbance at 650nm
4
3
2
1
0
Bispecific scFv-Cκ-scFv
PRb-CC01/cotinine
PRb-CN01/cotinine
PRb-CC02/cotinine
PRb-CC03/cotinine
Anti-HER2/cotinine
Anti-HER2/HER2

Fig. 4. Reactivity of anti-mPDGFRβ/cotinine scFv-Cκ-scFv fusion proteins. (A) mPDGFRβ-Fc chimera-coated microtiter plates were incubated with various concentrations of bispecific PRb-CC01 (●); PRb-CN01 (■); PRb-CC02 (▲); PRb-CC03 (▼); negative control (◆) complexed with cotinine scFv-Cκ-scFv fusion proteins. Wells were subsequently probed with HRP-conjugated anti-human Cκ antibody, and the amount of bound antibody was determined using TMB substrate solution. Results are shown as mean ± SD from duplicate experiments. (B) TNFα receptor extracellular domain-human Fc fusion protein served as a negative control antigen in an enzyme immunoassay. (C) To confirm reactivity of bispecific scFv-Cκ-scFv fusion proteins to cotinine, microtiter plates coated with cotinine-BSA were incubated with bispecific scFv-Cκ-scFv fusion proteins, and the amount of bound bispecific fusion protein was determined using HRP-conjugated anti-human Cκ antibody and TMB substrate solution. (D) To confirm simultaneous binding of bispecific scFv-Cκ-scFv fusion proteins to cotinine and mPDGFRβ, microtiter wells coated with cotinine-BSA was incubated with mPDGFRβ-Fc chimera, HRP-conjugated anti-human Fc antibody, and TMB substrate solution. Results are shown as the mean ± SD from triplicate experiments. ***$p < 0.001$ compared to controls.

To characterize the binding of anti-mPDGFRβ/cotinine scFv-Cκ-scFv fusion proteins in the presence of mPDGF-BB, a competition enzyme immunoassay was developed. Serially diluted bispecific scFv-Cκ-scFv fusion proteins with or without mPDGF-BB were added to wells coated with mPDGFRβ-Fc chimera fusion proteins. Next, HRP-conjugated anti-human Cκ antibodies and TMB substrate were added sequentially to the wells. Reactivity of clones PRb-CC01, PRb-CC02, and PRb-CC03, was inhibited in the presence of mPDGF-BB (Fig. 5A), although clone PRb-CN01 retained its binding activity to mPDGFRβ-Fc chimera protein in the presence of mPDGF-BB. We also performed flow cytometry to confirm the reactivity of individual clones to mPDGFRβ expressing NIH3T3 cells in the presence of mPDGF-BB and found that bispecific scFv-Cκ-scFv fusion proteins and biotin-labeled mPDGF-BB bound successfully to the cells. Similar to results from the competition enzyme immunoassay, only PRb-CN01 reacted to the cell surface mPDGFRβ in the presence of mPDGF-BB-biotin (Fig. 5B); reactivity of the other three clones was significantly hindered by mPDGF-BB. We also performed flow cytometry of bispecific scFv-Cκ-scFv fusion proteins to mPDGFRβ negative MOLT-4 cells and found that both PRb-CN01 and anti-HER2 bispecific scFv-Cκ-scFv fusion proteins did not bind to the cells (Fig. 6).

A

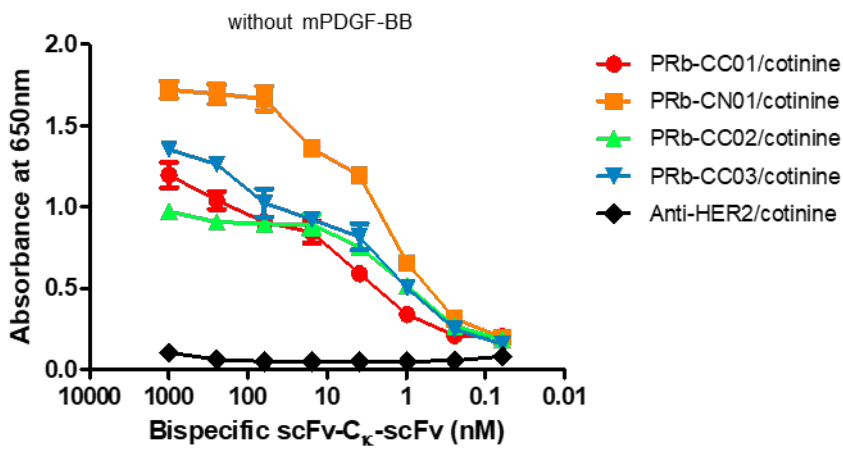
without mPDGF-BB
Absorbance at 650nm
2.0
1.5
1.0
0.5
0.0
10000
1000
100
10
1
0.1
0.01
Bispecific scFv-Cκ-scFv (nM)
PRb-CC01/cotinine
PRb-CN01/cotinine
PRb-CC02/cotinine
PRb-CC03/cotinine
Anti-HER2/cotinine

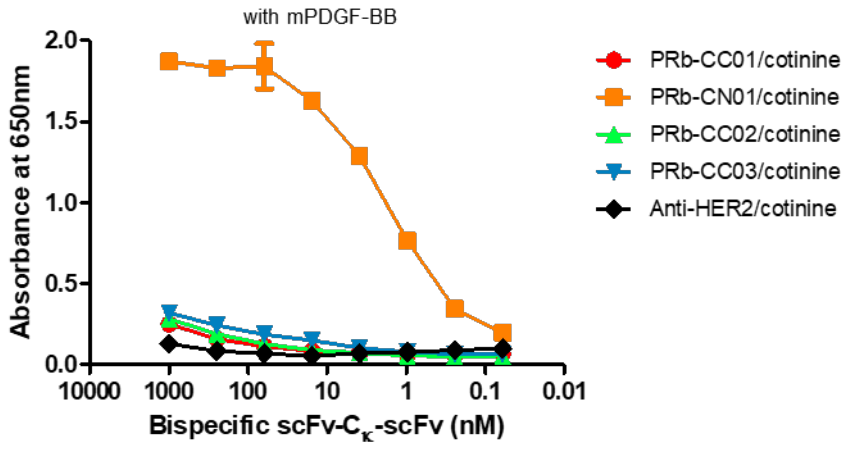
with mPDGF-BB
Absorbance at 650nm
2.0
1.5
1.0
0.5
0.0
10000
1000
100
10
1
0.1
0.01
Bispecific scFv-Cκ-scFv (nM)
PRb-CC01/cotinine
PRb-CN01/cotinine
PRb-CC02/cotinine
PRb-CC03/cotinine
Anti-HER2/cotinine

B

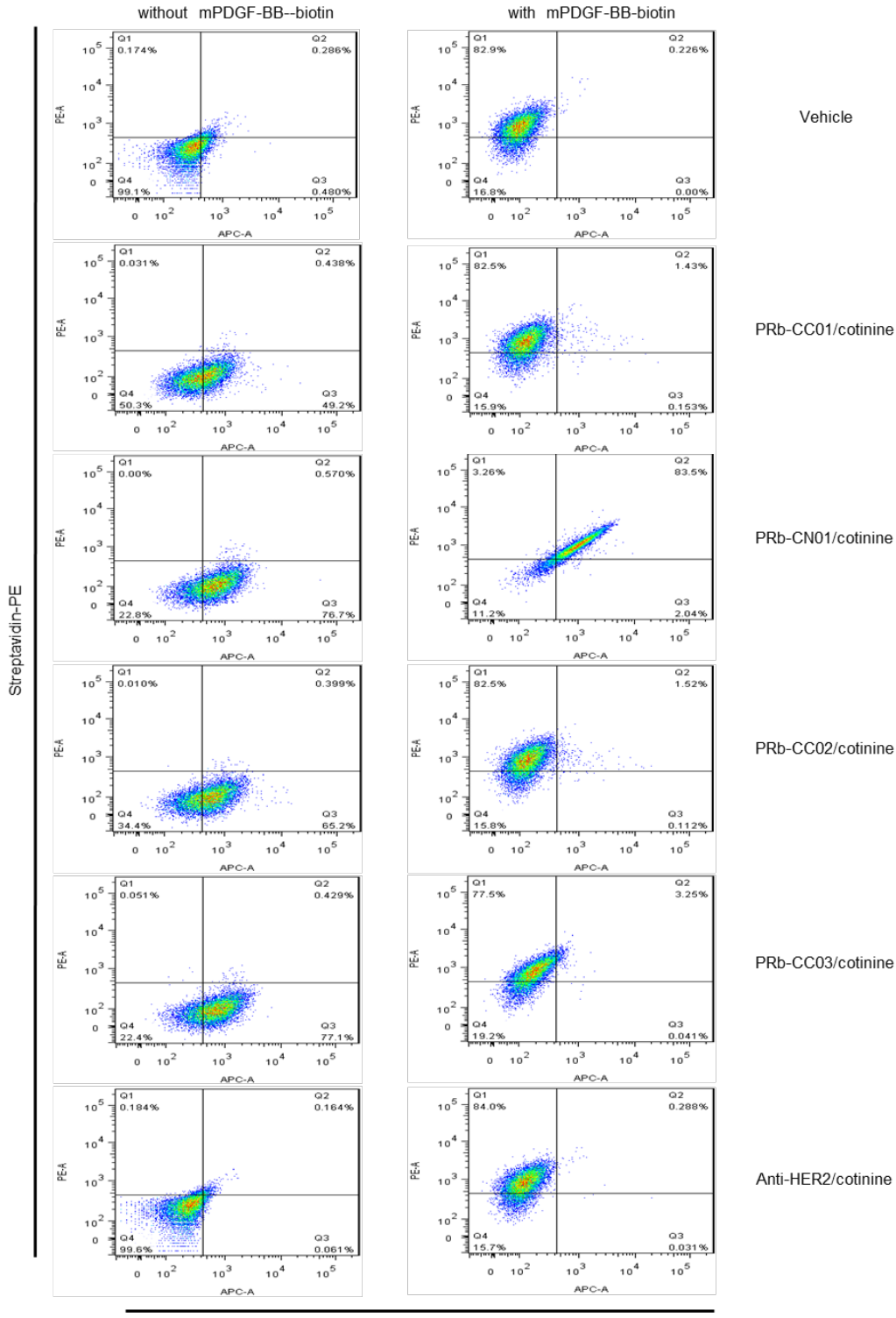
without mPDGF-BB--biotin
with mPDGF-BB-biotin
Vehicle
PRb-CC01/cotinine
PRb-CN01/cotinine
PRb-CC02/cotinine
PRb-CC03/cotinine
Anti-HER2/cotinine
Streptavidin-PE
APC-conjugated anti-human C_κ antibody
PE-A
APC-A
Q1 0.174%
Q2 0.286%
Q4 99.1%
Q3 0.480%
Q1 82.9%
Q2 0.226%
Q4 16.8%
Q3 0.00%
Q1 0.031%
Q2 0.438%
Q4 50.3%
Q3 49.2%
Q1 82.5%
Q2 1.43%
Q4 15.9%
Q3 0.153%
Q1 0.00%
Q2 0.570%
Q4 22.8%
Q3 76.7%
Q1 3.26%
Q2 83.5%
Q4 11.2%
Q3 2.04%
Q1 0.010%
Q2 0.399%
Q4 34.4%
Q3 65.2%
Q1 82.5%
Q2 1.52%
Q4 15.8%
Q3 0.112%
Q1 0.051%
Q2 0.429%
Q4 22.4%
Q3 77.1%
Q1 77.5%
Q2 3.25%
Q4 19.2%
Q3 0.041%
Q1 0.184%
Q2 0.164%
Q4 99.6%
Q3 0.061%
Q1 84.0%
Q2 0.288%
Q4 15.7%
Q3 0.031%

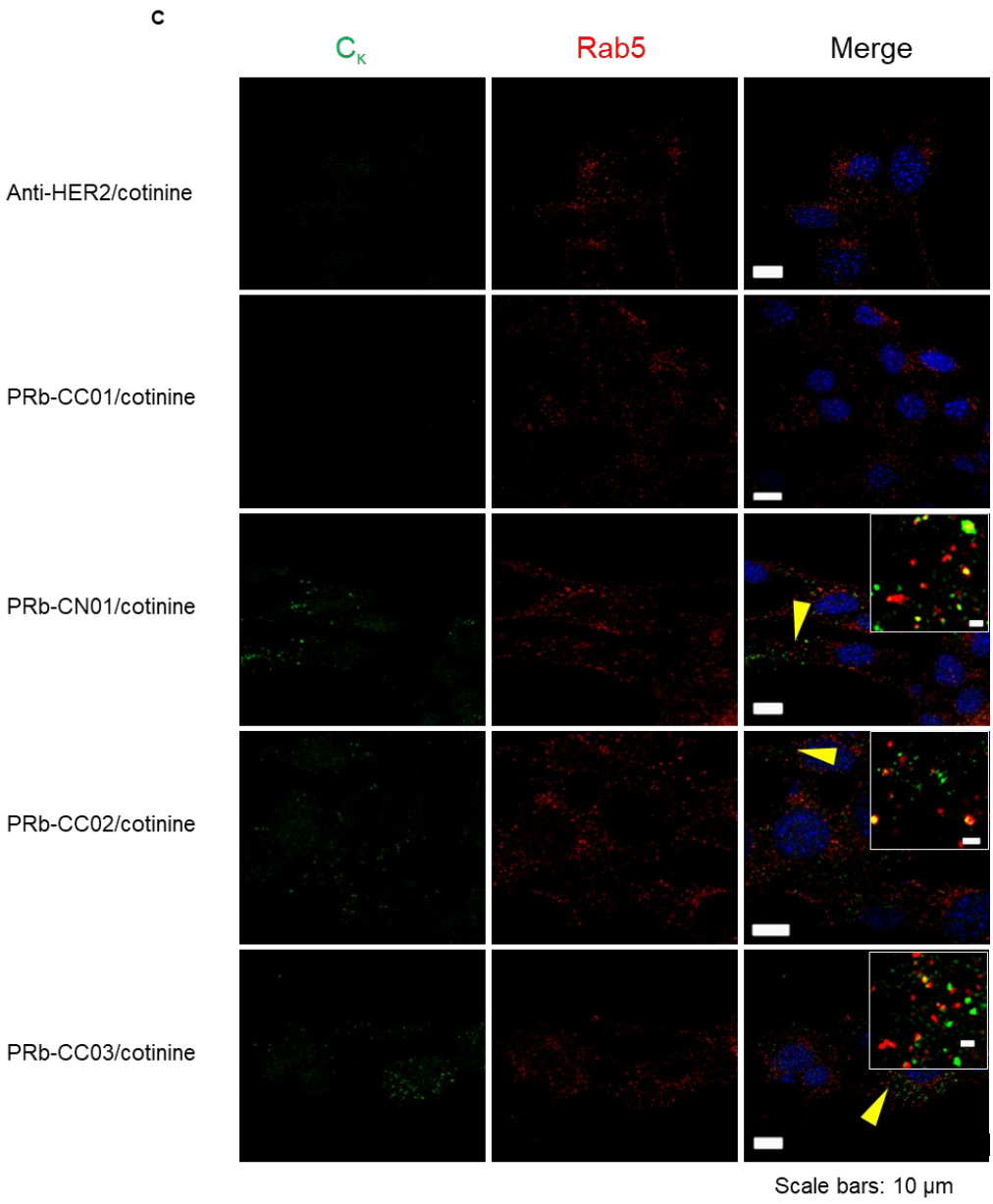
c
C_K
Rab5
Merge
Anti-HER2/cotinine
PRb-CC01/cotinine
PRb-CN01/cotinine
PRb-CC02/cotinine
PRb-CC03/cotinine
Scale bars: 10 μm

Fig. 5. Competition of anti-mPDGFRβ/cotinine scFv-Cκ-scFv fusion proteins with PDGF-BB and its cellular internalization. (A) mPDGFRβ-Fc chimera-coated microtiter plates were incubated with bispecific scFv-Cκ-scFv fusion proteins without (top) or with (bottom) mPDGF-BB (100 nM), and the amount of bound bispecific fusion protein was determined using HRP-conjugated anti-human Cκ antibody and TMB substrate solution. (B) mPDGFRβ-expressing NIH3T3 cells were treated with bispecific scFv-Cκ-scFv fusion proteins (100 nM) in flow cytometric assay buffer without or with mPDGF-BB-biotin. Cells were probed with APC-conjugated anti-human Cκ antibody and streptavidin-PE. Bispecific anti-HER2/cotinine scFv-Cκ-scFv fusion protein was used as a negative control. (C) Confocal microscopy enabled visualization of bispecific scFv-Cκ-scFv fusion protein internalization. NIH3T3 cells were incubated with fusion proteins, and surface-bound antibodies were removed. After cell fixation, fusion proteins were stained with FITC-conjugated anti-human Cκ antibody (green). To image the early endosome, cells were incubated with anti-Rab5 antibodies followed by staining with Alexa Fluor 546-conjugated goat anti-rabbit IgG (red). Areas indicated by arrows are shown at higher magnification in the inserts and show co-localization of anti-mPDGFRβ/cotinine scFv-Cκ-scFv fusion proteins and early endosomes. DNA was stained with DAPI (blue). Images were merged after initial capture. Scale bar, 10 μm.

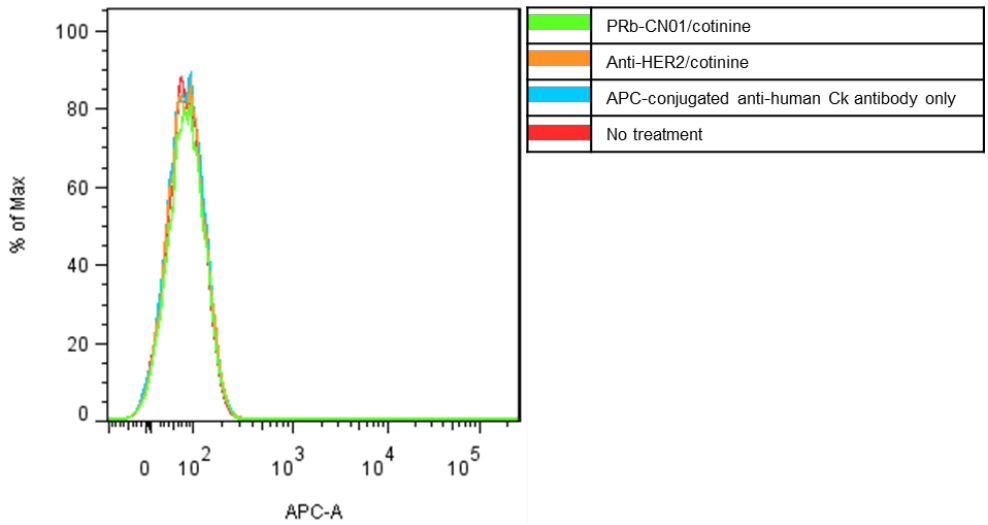

Fig. 6. Flow cytometry analysis on reactivity of bispecific anti-mPDGFRβ/cotinine scFv-Cκ-scFv fusion proteins on mPDGFRβ negative cells. MOLT-4 cells were incubated with bispecific anti-mPDGFRβ/cotinine scFv-Cκ-scFv fusion proteins (100 nM) and probed with APC-conjugated anti-human Cκ antibody (clone TB28-2, BD Biosciences, San Jose, CA, USA).

3. 4. Three anti-mPDGFRβ/cotinine scFv-Cκ-scFv fusion proteins undergo cellular internalization via endosomes.

To detect intracellular localization of the bispecific scFv-Cκ-scFv fusion proteins, NIH3T3 cells were incubated with anti-mPDGFRβ/cotinine scFv-Cκ-scFv and visualized with confocal microscopy after incubation with FITC-conjugated anti-human Cκ antibody and endosome-specific antibodies in parallel. Intracellular fluorescence was observed in cells incubated with PRb-CN01, PRb-CC02, and PRb-CC03 (Fig. 5C). When images were merged, we observed the same three fusion proteins co-localizing with endosome-specific antibodies.

3. 5. Anti-mPDGFRβ/cotinine scFv-Cκ-scFv fusion proteins complexed with cotinine-duocarmycin conjugates (cot-duo and cot-duo-cot) exert potent anti-proliferative effects on PDGFRβ expressing murine fibroblasts.

To measure cytotoxicity of the four anti-mPDGFRβ/cotinine scFv-Cκ-scFv fusion proteins complexed with cotinine-duocarmycin conjugates (cot-duo and cot-duo-cot), NIH3T3 cells were incubated with the complexes with or without mPDGF-BB, and cellular ATP content was analyzed to indicate relative cell viability. Cytotoxicity of bispecific scFv-Cκ-scFv fusion protein was defined as IC50 (table 1).

Table 1. In vitro potencies and 95% confidence intervals (CI) of bispecific anti-mPDGFRβ/cotinine scFv-Cκ-scFv fusion protein complexed cotinine-duocarmycin conjugates

	Cot-duo		Cot-duo-cot	
Bispecifi anti-PDGFRβ/cotinine scFv-Cκ	IC50 (nM)	95% CI	IC50 (nM)	95% CI
PRb-CC01				
with mPDGF-BB	27.1	19.1 - 38.5	67.2	52.0 - 86.9
without mPDGF-BB	25.0	18.1 - 34.7	87.6	54.4 - 141.1
PRb-CN01				
with mPDGF-BB	9.7	8.4 - 11.1	30.5	25.1 - 37.1
without mPDGF-BB	6.3	5.1 - 7.9	20.1	13.8 - 29.4
PRb-CC02				
with mPDGF-BB	20.6	16.2 - 26.3	69.0	54.2 - 87.9
without mPDGF-BB	20.1	15.2 - 26.5	125.4	47.4 - 328.7
PRb-CC03				
with mPDGF-BB	20.7	15.7 - 27.3	50.2	39.5 - 63.9
without mPDGF-BB	27.3	8.9 - 84.3	67.3	39.0-116.2
Anti-HER2				
with mPDGF-BB	23.2	17.4 - 31.0	60.8	48.4 - 76.4
without mPDGF-BB	36.7	27.9 - 48.3	93.7	55.3 -158.9
Cotinine duocarmycin conjugates				
with mPDGF-BB	22.8	16.6 - 31.4	56.7	44.3 - 72.6
without mPDGF-BB	15.5	11.7 - 20.3	45.4	29.8 - 69.2
Free duocarmycin				
with mPDGF-BB	23.8	18.2 - 31.0	60.3	41.1 - 88.5
without mPDGF-BB	9.7	7.3 - 12.9	35.7	23.4 - 54.4

Among the four tested proteins, PRb-CN01 showed significantly higher cytotoxicity in the presence and absence of mPDGF-BB compared to the control anti-HER2/cotinine scFv-Cκ-scFv fusion protein ($p < 0.01$; Fig. 7). PRb-CC02 and PRb-CC03 exhibited cytotoxicity but not significantly higher than that of control anti-HER2/cotinine scFv-Cκ-scFv fusion protein or non-internalizing PRb-CC01. However, the cotinine-duocarmycin conjugates became significantly ($p < 0.01$) more potent than free duocarmycin after forming a complex with PRb-CN01 in the presence of mPDGF-BB. As a control experiment, cytotoxicity of bispecific scFv-Cκ-scFv fusion protein complexed with cotinine-duocarmycin conjugates were tested against mPDGFRβ negative MOLT-4 cells. PRb-CN01 was not significantly more potent than the control anti-HER2/cotinine scFv-Cκ-scFv fusion proteins (Fig. 8).

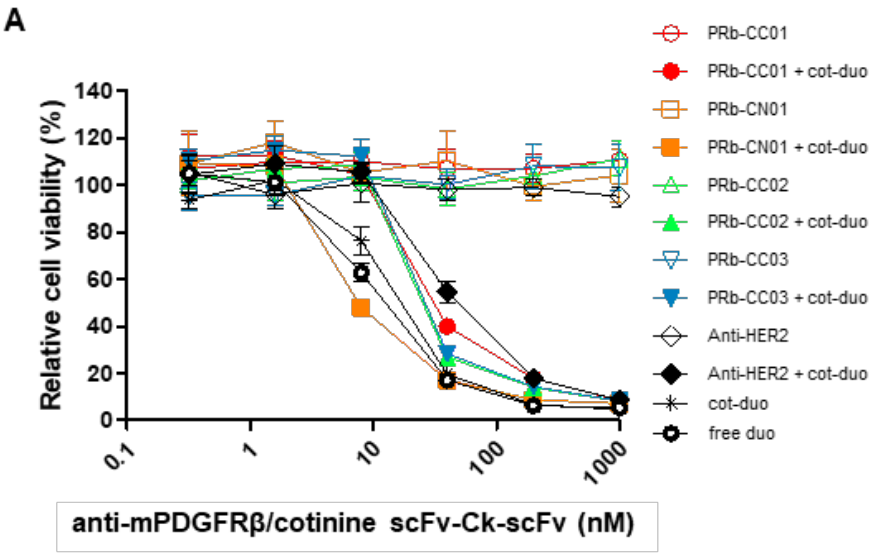
A
Relative cell viability (%)
140
120
100
80
60
40
20
0
0.1
1
10
100
1000
anti-mPDGFRβ/cotinine scFv-Ck-scFv (nM)
PRb-CC01
PRb-CC01 + cot-duo
PRb-CN01
PRb-CN01 + cot-duo
PRb-CC02
PRb-CC02 + cot-duo
PRb-CC03
PRb-CC03 + cot-duo
Anti-HER2
Anti-HER2 + cot-duo
cot-duo
free duo

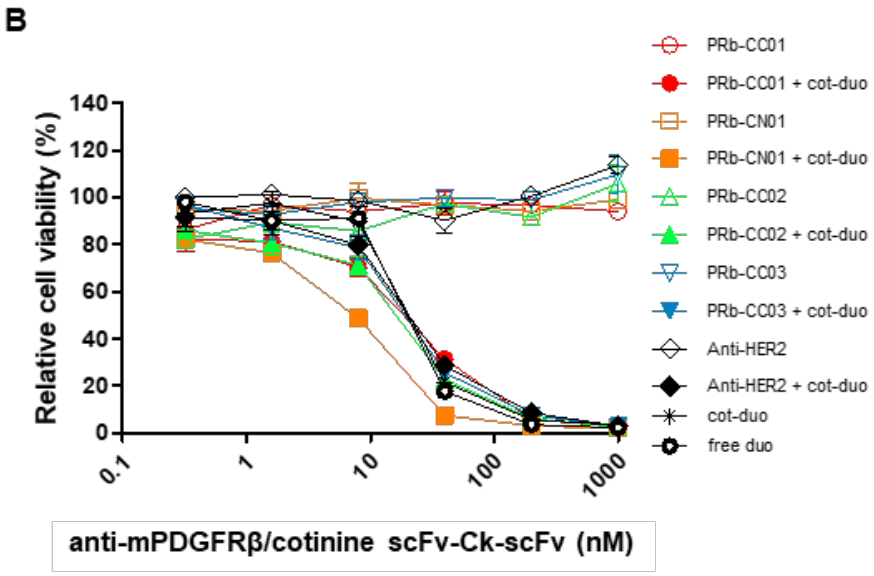
B
Relative cell viability (%)
140
120
100
80
60
40
20
0
0.1
1
10
100
1000
anti-mPDGFRβ/cotinine scFv-Ck-scFv (nM)
PRb-CC01
PRb-CC01 + cot-duo
PRb-CN01
PRb-CN01 + cot-duo
PRb-CC02
PRb-CC02 + cot-duo
PRb-CC03
PRb-CC03 + cot-duo
Anti-HER2
Anti-HER2 + cot-duo
cot-duo
free duo

C

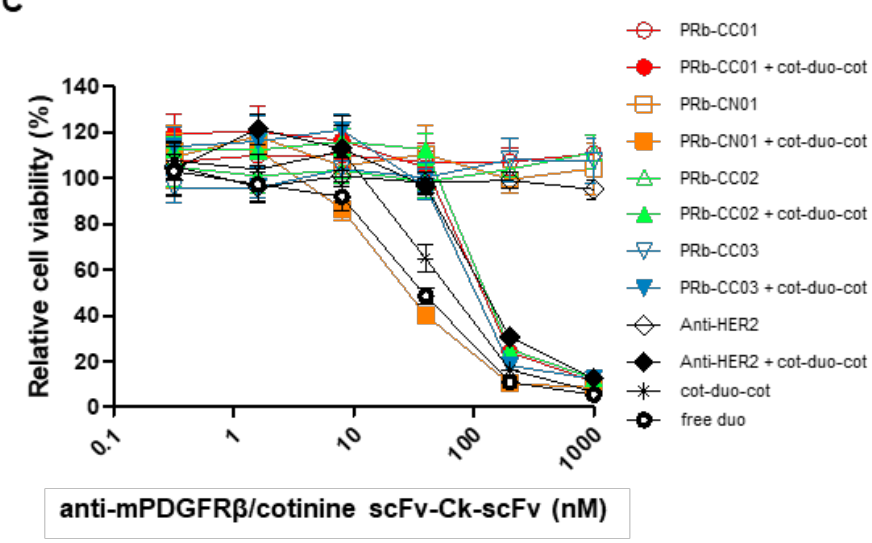
Relative cell viability (%)
140
120
100
80
60
40
20
0
0.1
1
10
100
1000
anti-mPDGFRβ/cotinine scFv-Ck-scFv (nM)
PRb-CC01
PRb-CC01 + cot-duo-cot
PRb-CN01
PRb-CN01 + cot-duo-cot
PRb-CC02
PRb-CC02 + cot-duo-cot
PRb-CC03
PRb-CC03 + cot-duo-cot
Anti-HER2
Anti-HER2 + cot-duo-cot
cot-duo-cot
free duo

D

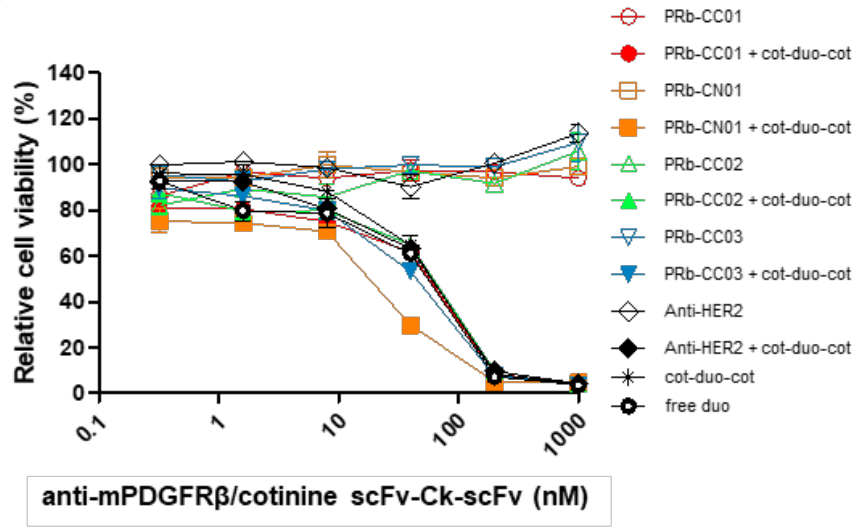
Relative cell viability (%)
140
120
100
80
60
40
20
0
0.1
1
10
100
1000
anti-mPDGFRβ/cotinine scFv-Ck-scFv (nM)
PRb-CC01
PRb-CC01 + cot-duo-cot
PRb-CN01
PRb-CN01 + cot-duo-cot
PRb-CC02
PRb-CC02 + cot-duo-cot
PRb-CC03
PRb-CC03 + cot-duo-cot
Anti-HER2
Anti-HER2 + cot-duo-cot
cot-duo-cot
free duo

Fig. 7. Cytotoxicity assays of bispecific anti-mPDGFRβ/cotinine scFv-Cκ-scFv fusion protein complexed with cotinine-duocarmycin conjugates against mPDGFRβ-expressing cells. (A) NIH3T3 cells were treated with the bispecific scFv-Cκ-scFv fusion protein and cot-duo without mPDGF-BB. Cellular ATP levels were measured to determine relative cell viability. Bispecific anti-HER2/cotinine scFv-Cκ-scFv fusion protein was used as a negative control. (B) The assay was repeated with mPDGF-BB. (C) NIH3T3 cells were treated with bispecific anti-mPDGFRβ/cotinine scFv-Cκ-scFv fusion protein and cot-duo-cot without mPDGF-BB. (D) The assay was repeated with mPDGF-BB. DMSO was used as a vehicle control for both cot-duo and cot-duo-cot. Results are shown as the mean ± SD from triplicate experiments.

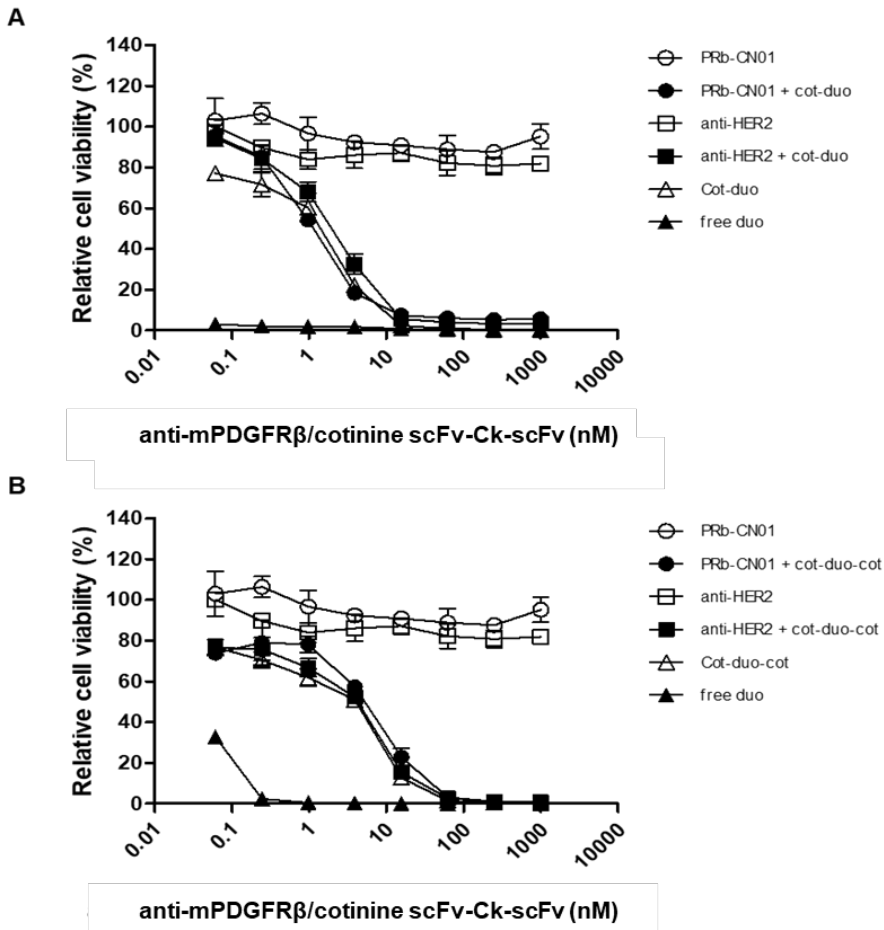

Fig. 8. Cytotoxicity assays of bispecific anti-mPDGFRβ/cotinine scFv-Cκ-scFv fusion protein complexed with cotinine-duocarmycin conjugates on mPDGFRβ negative cells. (A) MOLT-4 cells were treated with anti-mPDGFRβ x cotinine fusion protein and cot-duo (DAR4). Cellular ATP levels were measured to determine relative cell viability. (B) MOLT-4 cells were treated with bispecific anti-mPDGFRβ x cotinine scFv-Cκ-scFv and cot-duo-cot (DAR2). Bispecific anti-HER2 x cotinine scFv-Cκ-scFv fusion protein was used as a negative control. DMSO was used as a vehicle control of cotinine-duocarmycin conjugates. Results are shown as the mean ± SD acquired from triplicate experiments.

3. 6. Anti-mPDGFRβ/cotinine scFv-Cκ-scFv fusion proteins complexed with cot-duo inhibits neovascularization *in vivo*

In mouse model of laser-induced CNV, PRb-CN01/cotinine scFv-Cκ-scFv fusion protein complexed with cot-duo inhibited neovascularization (Fig. 9).

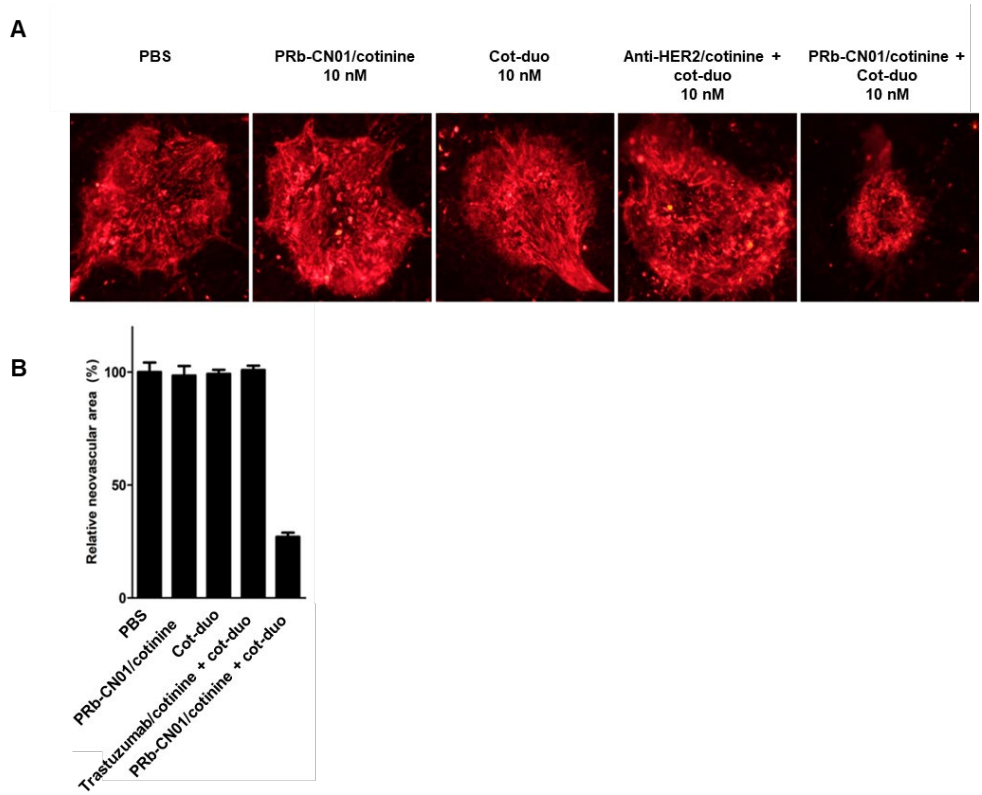

Fig. 9. Bispecific anti-mPDGFRβ/cotinine scFv-Cκ-scFv fusion proteins complexed with cot-duo inhibits neovascularization in laser-induced choroidal neovascularization (CNV) mouse model. (A) Representative photographs of CNV at 7 days after laser photocoagulation and intravitreal injection of PBS, PRb-CN01/cotinine, cot-duo, Anti-HER2/cotinine complexed with cot-duo, or PRb-CN01/cotinine complexed with cot-duo. Demonstrated by immunostaining with isolectin B4-594. (B) Quantitative demonstration of relative CNV areas regarding Fig. 9A.

4. Discussion

In this study, we tested a novel ADC development platform composed of bispecific scFv-Cκ-scFv fusion protein, and cotinine-cytotoxic drugs to determine its ability to simplify the selection process of optimal ADC antibodies and drug pairs. Ideally, it is practical to select antibody guaranteeing efficient internalization and release of cytotoxic drugs. But as the generation of individual ADC molecule using candidate antibodies requires a significant work of optimization and characterization including DAR, the antibodies have been frequently selected being based on their speed and efficiency of internalization at its initial screening phase. Moreover, an increased understanding of ADC cellular processing indicates internalization of antibody is not the sole factor determining an ADC's efficacy.

Endocytosis can occur through receptor-dependent and -independent mechanisms, including clathrin-mediated, caveolae-mediated, and clathrin-caveolin-independent endocytosis [40]. Clathrin-mediated endocytosis is the central route utilized by various ADCs [41], although some molecules are not restricted to a single pathway. After formation of a clathrin-coated vesicle, the ADC is subjected to endo-lysosomal trafficking [42], which requires uncoating of the vesicle by the Hsp70 complex and fusion with an early endosome. Endosomal and lysosomal ATP-dependent proton pumps cause gradual acidification from pH 6.0-6.2 to 4.5-5.0 [43] that frequently results in dissociation of ligands, such as insulin, epidermal growth factor (EGF), and low-density lipoprotein, from receptors in early endosomes and transport of the empty receptors to the cell membrane via the recycling compartment of narrow tubules.

Recycling of membrane proteins occurs through complex process by utilization of

Rab proteins/GTPases to regulate protein balance at the surface membrane [44, 45, 46, 47]. It is well known that antigen-ADC complex can be recycled to the cell surface and end up with significant amount of ADC returning to the cell surface [48]. This recycling can be influenced by the type of the ligand and where ADC binds the receptor. For example, EGF induces receptor degradation, while TGFα triggers recycling [49]. Early endosomes mature into late endosomes concomitant with protein loss, which plays a vital role in recycling. Late endosomes then fuse with lysosomes, where their acidity and enzymatic activities result in the ADC's release of the cytotoxic drugs from the antibody, either by cleavage of the linker or by antibody backbone degradation. Accumulation of the released drug in the cell depends on multiple events, including internalization, recycling, and endo-lysosomal trafficking of the receptor and subsequent linker/antibody proteolysis. Thus, the optimal antibody of an ADC should be selected based on its cytotoxicity tested in a format similar to the final molecule.

Classically, a secondary antibody conjugated with cytotoxic drug has been used to select internalizing and cytotoxic antibody clones using hybridoma culture supernatant [50], but stoichiometry between the primary antibody and the secondary antibody-cytotoxic drug conjugate can be difficult to control, especially when the primary antibody interacts with its target on the cell surface. In addition, antibody complex-induced in vitro polymerization and artificial internalization of the receptors may occur, which is difficult to predict or replicate in the real biological setting of an ADC. Decreased internalization of the complex due to receptor shedding may also take place. The antibody-hapten-cytotoxic drug complex provides a suitable model replicating an actual ADC molecule, and cytotoxic drugs with

various DARs can be combined with the bispecific antibody for broad cytotoxicity testing and comparisons.

To achieve this goal, the hapten should be absent from the biological system and nontoxic. Cotinine is a small molecule with a weight of 176.22 g/mol not found in human or animal tissues [51] which is commonly used as a biomarker for smoking exposure. Cotinine is nontoxic and has an LD50 of 4 ± 0.1 g/kg in mice [29]. Furthermore, no deleterious side effects were induced in humans treated with up to 1,800 mg cotinine daily for four consecutive days [52]. In our previous study, we generated a high affinity, anti-cotinine antibody with k_{on}, k_{off}, and K_D values of $2.6 \times 10^{6}M^{-1}s^{-1}$, $1.3 \times 10^{-5}s^{-1}$, and $4.9 \times 10^{-12}M$, respectively [51]. This antibody specifically binds cotinine and does not cross-react with small molecules structurally similar to cotinine, such as anabasine, cholesterol, nicotine, and caffeine. Furthermore, the antibody's reactivity was confirmed in various configurations, including conventional IgG, scFv, tandem scFv Fc fusion, bispecific scFv-Cκ-scFv fusion protein, and tetravalent bispecific antibody [30, 31, 33, 39].

At first in in vivo setting, we applied the complex of anti-cotinine antibody and cotinine-conjugated anti-tumor molecule to a tumor xenograft model. In mice, the half-life of cotinine-conjugated anti-vascular endothelial growth factor aptamer and anti-cotinine IgG complex in the mice was determined to be 15 h [53]. This complex showed a significant anti-tumor effect comparable to clinically available anti-vascular endothelial growth factor (VEGF) antibody. Then we generated ADC made with the tetravalent bispecific anti-EGFR x cotinine antibody in IgG-scFv format. When complexed with cot-biotin-cot peptide with 12 amino acid residues between two cotinine conjugated at the amino and carboxy termini of the peptide, the half-

life of this IgG-scFv and cot-biotin-cot peptide were determined to be 18 h in mice. As the amino acid length of the cot-biotin-cot peptide significantly affected the half-life of the complex, the bivalent nature of the complex formation was critical for the half-life [39]. The complex of cot-duo-cot and anti-EGFR x cotinine antibody in IgG-scFv format showed a significant anti-tumor effect.

Interestingly, we observed that there is a little difference between the cytotoxicity of free duocarmycin and cotinine-duocarmycin conjugate in in vitro setting (Fig. 7). The complex formation between anti-HER2/cotinine scFv-Cκ-scFv fusion protein and cotinine-duocarmycin conjugate lowered the toxicity of duocarmycin in vitro, implying that the fusion protein forms a complex with the drug, decreasing uptake of the drug into the cells. In the in vivo experiments using the tetravalent bispecific antibody, there were no significant weight loss in mice injected with cotinine-duocarmycin conjugate mixed with negative-control IgG, although duocarmycin has been previously reported to induce significant weight loss in mice [54]. A possible explanation is a rapid clearance of liberated cotinine-duocarmycin from the bloodstream, minimizing systemic exposure. This observation opens the possibility for introducing various forms of linkers between cotinine and toxin and making the release of toxin from cotinine only in tumor environment, for example by the metalloprotease. Furthermore, it could be combined with non-internalizing antibody binding to targets abundant in tumor environment to make a new form of non-internalizing ADC with maximized by-stander effect [55, 56]. As the cotinine-drug conjugates are released from the tumor environment without degradation, it would be rapidly cleared from the bloodstream without damaging normal cells.

Excessive signaling between PDGF and PDGFR plays an important role in many

cancers, such as renal cell carcinoma, lung cancer, glioblastoma, chronic monomyelocytic leukemia, and prostate cancer [57]. PDGFR stimulates tumor growth in both autocrine and paracrine manners by directly affecting tumor growth, related blood vessels, and stromal fibroblasts to promote tumor persistence [58]. The PDGF family consists of monomeric PDGF-A, -B, -C and -D and dimeric PDGF-AA, -AB, -BB, -CC and -DD. PDGFs bind receptor tyrosine kinases PDGF receptor-α and -β, which dimerize upon binding the PDGF dimer, leading to three possible receptor combinations (αα, ββ, and αβ). The extracellular region of the receptors consists of five immunoglobulin-like domains, while the intracellular region contains a tyrosine kinase domain. The ligand-binding sites of the receptors are located in the first three immunoglobulin-like domains. PDGF-CC specifically interacts with PDGFR-αα and -αβ, but not with -ββ, and thereby resembles PDGF-AB. PDGF-DD binds PDGFR-ββ with high affinity and PDGFR-αβ to a markedly lower extent and is therefore considered PDGFR-ββ specific. PDGF-AA binds only PDGFR-αα, and PDGF-BB is the only PDGF that can bind all three receptor combinations with high affinity. PDGF binds to immunoglobulin like domains 2 and 3 of PDGFR, inducing dimerization of the receptor followed by direct receptor-receptor interaction involving immunoglobulin-like domains 4 and 5 for further stabilization. Subsequently, the ligand-receptor complex undergoes internalization [59]. While the cytotoxicity of PRb-CN01 complexed with cot-duo or cot-duo-cot was still high even after addition of mPDGF-BB, addition of mPDGF-BB slightly reduced that of three mPDGF-BB competitive (PRb-CC01, PRb-CC02 and PRb-CC03) fusion proteins complexed with either cot-duo or cot-duo-cot (Fig. 7). The mPDGF-BB might have bound to the PDGFRβ already bound to PRb-CN01,

enhancing the internalization of the receptor, promoting the cytotoxic effect of cot-duo and cot-duo-cot. In the later cases, mPDGF-BB would promote cell proliferation. In our study, construct PRb-CN01 did not compete with PDGF-BB (Fig. 5) but did induce cytotoxicity independent of PDGF-BB (Fig. 7). We also tried to stimulate PDGFRβ dimerization by adding cot-duo-cot, but cytotoxicity of the bispecific antibody was reduced, and we could not determine if cot-duo-cot actually induced PDGFRβ dimerization. Recently, an interaction between VEGF-A and PDGFRβ was observed with a K_D of 340 pM [60], and VEGFR2 and PDGFRβ can form complexes on pericyte surfaces [61, 62]. These cross-family interactions can provide another potential mechanism of PDGFRβ internalization. One monoclonal antibody targeting PDGF and PDGFR signaling has been approved for clinical use, and various biological agents, including antibodies and aptamers, are in active preclinical and clinical development [63]. Olaratumab (IMC-3G3, Lartruvo™) is a recombinant anti-PDGFRα human IgG1 antibody that specifically binds PDGFRα and blocks PDGF-AA, PDGF-BB, and PDGF-CC binding and receptor activation without cross-reacting with PDGFRβ [64]. Based on the results of a phase Ib/II study of advanced soft tissue sarcoma in which combination therapy of olaratumab and doxorubicin significantly improved median overall survival compared to doxorubicin alone [65], olaratumab first received approval for treating this cancer in the U.S. in October 2016 [66].

Two families of linkers, cleavable and non-cleavable, are commonly used for conjugation of cytotoxic drugs to antibody. Cleavable linkers utilize inherent properties of tumor cells to selectively deliver and release the cytotoxic drugs. Commonly used mechanisms involve protease, pH, and glutathione sensitivity [67].

The protease sensitive strategy relies on proteases found predominantly in tumor cell lysosomes for specific recognition and cleavage of linker peptides. For example, brentuximab vedotin, an FDA-approved ADC, consists of a valine-citrulline dipeptide that undergoes cleavage by lysosomal cathepsin B [11, 68]. Two FDA-approved ADCs are pH-sensitive: inotuzumab ozogamicin and gemtuzumab ozogamicin, which contain acid-labile 4-(4'-acetylphenoxy) butanoic acid linkers. This strategy exploits the lower endosomal pH compared to that of the cytosol [67] and often involves release of the drug via hydrolysis in the lysosome. The glutathione-sensitive strategy takes advantage of a higher intracellular glutathione concentration compared to that in plasma. In this case, cytotoxic drugs are released upon reduction of a disulfide bridge in the linker by glutathione [67]. Non-cleavable linkers release drugs only after complete degradation of the antibody after internalization. We have constructed cotinine conjugated valine-citrulline-PAB-duocarmycin, valine-citrulline-PAB-Monomethyl auristatin E (MMAE) or valine-citrulline-PAB-maleimidomethyl cyclohexane-1-carboxylate (mcc)-mertansine (DM1). We have tested DAR1 and DAR4 cotinine-cytotoxic drugs and discovered that DAR4 cotinine-cytotoxic drug was more potent than DAR1 and also discovered that duocarmycin was the most potent when conjugated to cotinine (data not shown). For this reason, we have only used cotinine-duocarmycin for detailed studies.

5. Conclusion

Bispecific anti-mPDGFRβ/cotinine scFv-Cκ-scFv fusion protein and cotinine-conjugated duocarmycin were successfully complexed to induce cytotoxicity in NIH3T3 cells expressing PDGFRβ and inhibited neovascularization in vivo. Our results indicate this platform can be used to select the ideal combination of internalizing antibody and cytotoxic drug during ADC development.

6. Reference

1. P.J. Carter, P.D. Senter, Antibody-drug conjugates for cancer therapy, Cancer. J. 14 (2008) 154-69.

2. R. Liu, R.E. Wang, F. Wang, Antibody-drug conjugates for non-oncological indications, Expert. Opin. Biol. Ther. 16 (2016) 591-53.

3. K. Strebhardt, A. Ullrich, Paul Ehrlich's magic bullet concept: 100 years of progress, Nat. Rev. Cancer. 8 (2008) 473-80.

4. J.M. Lambert, A. Berkenblit, Antibody-drug conjugates for cancer treatment, Annu. Rev. Med. 69 (2018) 191-207.

5. A. Beck, L. Goetsch, C. Dumontet C, N. Corvaia, Strategies and challenges for the next generation of antibody-drug conjugates, Nat. Rev. Drug. Discov. 16 (2017) 315-337.

6. K.J. Norsworthy, C.W. Ko, J.E. Lee, J. Liu, C.S. John, D. Przepiorka, A.T. Farrell, R. Pazdur, FDA approval summary: Mylotarg for treatment of patients with relapsed or refractory CD33-positive acute myeloid leukemia, Oncologist. 23 (2018) 1-6.

7. H.L. Perez, P.M. Cardarelli, S. Deshpande, S. Gangwar, G.M. Schroeder, G.D. Vite, R.M. Borzilleri, Antibody-drug conjugates: current status and future directions, Drug. Discov. Today. 19 (2014) 869-81.

8. C.R. Behrens, B. Liu, Methods for site-specific drug conjugation to antibodies, MAbs. 6 (2014) 46-53.

9. C.R. Behrens, E.H. Ha, L.L. Chinn, S. Bowers, G. Probst, M. Fitch-Bruhns, J. Monteon, A. Valdiosera, A. Bermudez, S. Liao-Chan, T. wong, J. Melnick, J.W. Theunissen, M.R. Flory, D. Houser, K. Venstrom, Z. Levashova, P.Sauer, T.S.

Migone, E.H. van der Horst, R.L. Halcomb, D.Y. Jackson, Antibody-Drug Conjugates (ADCs) derived from interchain cysteine cross-linking demonstrate improved homogeneity and other pharmacological properties over conventional heterogeneous ADCs, Mol. Pharm. 12 (2015) 3986-98.

10. N. Diamantis, U. Banerji, Antibody-drug conjugates—an emerging class of cancer treatments, Br. J. Cancer. 114 (2016) 362-6.

11. T. Riedl, E. van Boxtel, M. Bosch, P.W. Parren, A.F. Gerritsen, High-throughput screening for internalizing antibodies by homogeneous fluorescence imaging of a pH-activated probe, J. Biomol. Screen. 21 (2016) 12-23.

12. C.M. Boyer, L. Pusztai, J.R. Wiener, F.J. Xu, G.S. Dean, B.S. Bast, K.C. O'Briant, M. Greenwald, K.A. DeSombre, R.C. Bast Jr., Relative cytotoxic activity of immunotoxins reactive with different epitopes on the extracellular domain of the c-erbB-2 (HER-2/neu) gene product p185, Int. J. Cancer. 82 (1999) 525-31.

13. E. Nordberg, M. Friedman, L. Göstring, G.P. Adams, H. Brismar, F.Y. Nilsson, S. Ståhl, B. Glimelius, J. Carlsson, Cellular studies of binding, internalization and retention of radiolabeled EGFR-binding affibody molecule, Nucl. Med. Biol. 34 (2007) 609-18.

14. J.J. Lammerts van Bueren, W.K. Bleeker, H.O. Bøgh, M. Houtkamp, J. Schuurman, J.G. van de Winkel, P.W. Parren, Effect of target dynamics on pharmacokinetics of a novel therapeutic antibody against the epidermal growth factor receptor: implications for the mechanisms of action, Cancer. Res. 66 (2006) 7630-8.

15. M.M. Schmidt, G.M. Thurber, K.D. Wittrup, Kinetics of anti-carcinoembryonic antigen antibody internalization: effects of affinity, bivalency, and

stability, Cancer. Imunnol. Immunother. 57 (2008) 1879-90.

16. R.B. Michel, M.J. Mattes, Intracellular accumulation of the anti-CD20 antibody 1F5 in B-lymphoma cells, Clin. Cancer. Res. 8 (2002) 2701-13.17.

17. R.M. Perera, R. Zoncu, T.G. Johns, M. Pypaert, F.T. Lee, I. Mellman, L.J. Old, D.K. Toomre, A.M. Scott, Internalization, intracellular trafficking, and biodistribution of monoclonal antibody 806: a novel anti-epidermal growth factor receptor antibody, Neoplasia. 9 (2007) 1099-110.

18. A. Danielczyk, R. Stahn, D. Faulstich, A. Löffler, A. Märten, U. Karsten, S. Goletz, PankoMab: a potent new generation anti-tumor MUC1 antibody, Cancer. Immunol. Immunother. 55 (2006) 1337-47.

19. K. Klussman, B.J. Mixan, C.G. Cerveny, D.L. Meyer, P.D. Senter, A.F. Wahl, Secondary mAb—vcMMAE conjugates are highly sensitive reporters of antibody internalization via the lysosome pathway, Bioconjug. Chem. 15 (2004) 765-73.

20. K.R. Durbin, C. Phipps, X. Liao, Mechanistic modeling of antibody-drug conjugate internalization at the cellular level reveals inefficient processing steps, Mol. Cancer. Ther. 17 (2018) 1341-1351.

21. J. Paulsson, T. Sjöblom, P. Micke, F. Pontén, G. Landberg, C.H. Heldin, J. Bergh, D.J. Brennan, K. Jirström, A. Ostman, Prognostic significance of stromal platelet-derived growth factor beta-receptor expression in human breast cancer, Am. J. Pathol. 175 (2009) 334-41.

22. N. Jo, C. Mailhos, M. Ju, E. Cheung, J. Bradley, K. Nishijima, G.S. Robinson, A.P. Adamis, D.T. Shima, Inhibition of platelet-derived growth factor B signaling enhances the efficacy of anti-vascular endothelial growth factor therapy in

multiple models of ocular neovascularization, Am. J. Pathol. 168 (2006) 2036-53.

23. K. Strittmatter, H. Pomeroy, A.G. Marneros, Targeting platelet-derived growth factor receptor β(+) scaffold formation inhibits choroidal neovascularization, Am. J. Pathol. 186 (2016) 1890-9.

24. M. Lindborg, E. Cortez, I. Höidén-Guthenberg, E. Gunneriusson, E. von Hage, F. Syud, M. Morrison, L. Abrahmsén, N. Herne, K. Pietras, F.Y. Frejd, Engineered high-affinity affibody molecules targeting platelet-derived growth factor receptorβ in vivo, J. Mol. Biol. 407 (2011) 298-315.

25. V. Tolmachev, Z. Varasteh, H. Honarvar, S.J. Hosseinimehr, O. Eriksson, P. Jonasson, F.Y. Frejd, L. Abrahmsen, A. Orlova, Imaging of platelet-derived growth factor receptor β expression in glioblastoma xenografts using affibody molecule 111In-DOTA-Z09591, J. Nucl. Med. 55 (2014) 294-300.

26. Q. Shi, Z. Tao, H. Yang, Q. Fan, D. Wei, L. Wan, X. Lu, PDGFRβ-specific affibody-directed delivery of a photosensitizer, IR700, is efficient for vascular-targeted photodynamic therapy of colorectal cancer, Drug. Deliv. 24 (2017) 1818-1830.

27. X. Lin, K. Takahashi, Y. Liu, A. Derrien, P.O. Zamora, A synthetic, bioactive PDGF mimetic with binding to both alpha-PDGF and beta-PDGF receptors, Growth. Factors. 25 (2007) 87-93.

28. J. Pahara, H. Shi, X. Chen, Z. Wang, Dimerization drives PDGF receptor endocytosis through a C-terminal hydrophobic motif shared by EGF receptor, Exp. Cell. Res. 316 (2010) 2237-50.

29. O. Riah, J.C. Dousset, P. Courriere, J.L. Stigliani, G. Baziard-Mouysset, Y. Belahsen, Evidence that nicotine acetylcholine receptors are not the main targets of

cotinine toxicity, Toxicol. Lett. 109 (1999) 21-9.

30. S. Park, D. Hwang, J. Chung, Cotinine-conjugated aptamer/anti-cotinine antibody complexes as a novel affinity unit for use in biological assays, Exp. Mol. Med. 44 (2012) 554-61.

31. Y. Lee, H. Kim, J. Chung, An antibody reactive to the Gly63-Lys68 epitope of NT-proBNP exhibits O-glycosylation-independent binding, Exp. Mol. Med. 46 (2014) e114.

32. S.E. Reed, E.M. Staley, J.P. Mayginnes, D.J. Pintel, G.E. Tullis, Transfection of mammalian cells using linear polyethylenimine is a simple and effective mean sof producing recombinant adeno-associated virus vectors, J. Vriol. Methods. 138 (2006) 85-98.

33. S. Yoon, Y.H. Kim, S.H. Kang, S.K. Kim, H.K. Lee, H. Kim, J. Chung, I.H. Kim, Bispecific HER2 x cotinine antibody in combination with cotinine-(histidine)2-iodine for the pretargeting of HER2-positive breast cancer xenografts, J. Cancer. Res. Clin. Oncol. 140 (2014) 227-33.

34. M.S. Lee, J.C. Lee, C.Y. Choi, J. Chung, Production and characterization of monoclonal antibody to botulinum neurotoxin type B light chain by phage display, Hybridoma (Larchmt). 27 (2008) 18-24.

35. C.F. Barbas III, D.R. Burton, J.K. Scott, G.J. Silverman, Phage display- a laboratory manual, Cold Spring Harbor Laboratory Press, New York, 2001.

36. W. Yang, A. Yoon, S. Lee, S. Kim, J. Han, J. Chung, Next-generation sequencing enables the discovery of more diverse positive clones from a phage-displayed antibody library, Exp. Mol. Med. 49 (2017) e308.

37. S. Park, S.D. Kim, H.Y. Lee, D. Hwang, J.S. Park, Y.S. Bae, J. Chung, A

novel delivery platform for therapeutic peptides, Biochem. Biophys. Res. Commun. 450 (2014) 13-8.

38. J.M. Lim, K.S. Lee, H.A. Woo, D. Kang, S.G. Rhee, Control of the pericentrosomal H2O2 level by peroxiredoxin I is critical for mitotic progression, J. Cell. Biol. 210 (2015) 23.

39. J. Jin, G. Park, J.B. Park, S. Kim, H. Kim, J. Chung, An anti-EGFR x cotinine bispecific antibody complexed with cotinine-conjugated duocarmycin inhibits growth of EGFR-positive cancer cells with KRAS mutations, Exp. Mol. Med. 50 (2018) 67.

40. S.D. Conner, S.L. Schmid, Regulated portals of entry into the cells, Nature. 422 (2003) 37-44.

41. M. Kalim, J. Chen, S. wang, C. Lin, S. Ullah, K. Liang, Q. Ding, S. Chen, J. Zhan, Intracelular trafficking of new anticancer therapeutics: antibody-drug conjugates, Drug. Des. Devel. Ther. 11 (2017) 2265-2276.

42. S. Mukherjee, R.N. Ghosh, F.R. Maxfield, Endocytosis, Physiol. Rev. 77 (1997) 759-803.

43. T.M. Desai, M. Marin, C. Mason, G.B. Malikyan, pH regulation in early endosomes and interferon-inducible transmembrane proteins control avian retrovirus fusion, J. Biol. Chem. 292 (2017) 7817-7827.

44. O.A. Weisz, Acidification and protein traffic, Int. Rev. Cytol. 226 (2003) 259-319.

45. G. Scita, P.P. Di Fiore, The endocytic matrix, Nature. 463 (2010) 464-73.

46. J. Zhang, X. Zhang, G. Liu, D. Chang, X. Liang, X. Zhu, W. Tao, L. Mei, Intracellular trafficking network of protein nanocapsules: endocytosis, exocytosis

and autophagy, Theranostics. 6 (2016) 2099-2113.

47. B.D. Grant, J.G. Donaldson, Pathways and mechanisms of endocytic recycling, Nat. Rev. Mol. Cell. Biol. 10 (2009) 597-608.

48. K.R. Durbin, C. Phipps, X. Liao, Mechanistic modeling of antibody-drug conjugate internalization at the cellular level reveals inefficienct processing steps, Mol. Cancer. Ther. 17 (2018) 1341-1351.

49. K.E. Longva, F.D. Blystad, E. Stang, A.M. Larsen, L.E. Johannessen, I.H. Madshus, Ubiquitination and proteasomal activity is required for transport of the EGF receptor to inner membranes of multivesicular bodies, J. Cell. Biol. 156 (2002) 843-54.

50. K. Klussman, B.J. Mixan, C.G. Cerveny, D.L. Meyer, P.D. Senter, A.F. Wahl, Secondary mAb—vcMMAE conjugates are highly sensitive reporters of antibody internalization via the lysosome pathway, Bioconjug. Chem. 15 (2004) 765-73.

51. H. Kim, S. Yoon, J. Chung, In vitro and in vivo application of anti-cotinine antibody and cotinine-conjugated compounds, BMB. Rep. 47 (2014) 130-4.

52. I. Kim, M.A. Huestis, A validated method for the determination of nicotine, cotinine, trasn-3'-hydroxycotinine, and norcotinine in human plasma using solid-phase extraction and liquid chromatography-atmospheric pressure chemical ionization-mass spectrometry, J. Mass. Spectrom. 41 (2006) 815-21.

53. K. Heo, S.W. Min, H.J. Sung, H.G. Kim, H.J. Kim, Y.H. Kim, B.K. Choi, S. Han, S. Chung, E.S. Lee, J. Chung, I.H. Kim, An aptamer-antibody complex (oligobody) as a novel delivery platform for targeted cancer therapies, J. Control. Release. 229 (2016) 1-948.

54. G.A. Vielhauer, M. Swink, N.K. Parelkar, J.P. Lajiness, A.L. Wolfe, D. Boger, Evaluation of reductively activated duocarmycin prodrug against murine and human solid cancers, Cancer. Biol. Ther. 14 (2013) 527-36.

55. E. Perrino, M. Steiner, N. Krall, G.J. Bernardes, F. Pretto, G. Casi, D. Neri, Curative properties of noninternalizing antibody-drug conjugates based on maytansinoids, Cancer. Res. 74 (2014) 2569-78.

56. A. Dal Corso, S. Cazzamalli, R. Gébleux, M. Mattarella, D. Neri, Protease-cleavable linkers modulate the anticancer activity of noninternalizing antibody-drug conjugates, Bioconjug. Chem. 28 (2017) 1826-1833.

57. K. Pietras, T. Sjoblom, K. Rubin, C.H. Heldin, A. Ostman, PDGF receptors as cancer drug targets, Cancer. Cell. 3 (2003) 439-43.

58. A. Ostman, C.H. Heldin, PDGF receptors as targets in tumor treatment, Adv. Cancer. Res. 97 (2007) 247-74.

59. C.H Heldin, J. Lennartsson, B. Westermark, Involvement of platelet-derived growth factor ligands and receptors in tumorigenesis, J. Intern. Med. 283 (2018) 16-44.

60. S.B. Mamer, S. Chen, J.C. Weddell, A. Palasz, A. Wittenkeller, M. Kumar, P.I. Imoukhuede, Discovery of high-affinity PDGF-VEGFR interactions: Redefining RTK dynamics, Sci. Rep. 7 (2017) 16439.

61. J.I. Greenberg, D.J. Shields, S.G. Barillas, L.M. Acevedo, E. Murphy, J. Huang, L. Scheppke, C. Stockmann, R.S. Johnson, N. Angle, D.A. Cheresh, A role for VEGF as a negative regulator of pericyte function and vessel maturation, Nature. 456 (2008) 809-13.

62. J.I. Greenberg, D.A. Cheresh, VEGF as an inhibitor of tumor vessel

maturation: implications for cancer therapy, Expert. Opin. Biol. Ther. 9 (2009) 1347-56.

63. N. Papadopoulos, J. Lennartsson, The PDGF/PDGFR pathway as a drug target, Mol. Aspects. Med. 62 (2018) 75-88.

64. N. Loizos, Y. Xu, J. Huber, M. Liu, D. Lu, B. Finnerty, R. Rolser, A. Malikzay, A. Persaud, E. Corcoran, D.S. Deevi, P. Balderes, R. Bassi, X. Jimenez, C.J. Joynes, V.R. Mangalampalli, P. Steiner, J.R. Tonra, Y. Wu, D.S. Pereira, Z. Zhu, D.L. Ludwig, D.J. Hicklin, P. Bohlen, L. Witte, P. Kussie, Targeting the platelet-derived growth factor receptor alpha with a neutralizing human monoclonal antibody inhibits the growth of tumor xenografts: implications as a potential therapeutic target, Mol. Cancer. Ther. 4 (2005) 369-79.

65. W.D. Tap, R.L. Jones, B.A. Van Tine, B. Chmielowski, A.D. Elias, D. Adkins, M. Agulnik, M.M. Cooney, M.B. Livingston, G. Pennock, M.R. Hameed, G.D. Shah, A. Qin, A. Shahir, D.M. Cronier, R. Ilaria Jr., I. Conti, J. Cosaert, G.K. Schwartz, Olaratumab and doxorubicin versus doxorubicin alone for treatment of soft-tissue sarcoma: an open-label phase 1b and randomised phase 2 trial, Lancet. 388 (2016) 488-97.

66. M. Shirley, Olaratumab: First global approval, Drugs. 77 (2017) 107-112.

67. N. Jain, S.W. Smith, S. Ghone, B. Tomczuk, Current ADC linker chemistry, Pharm. Res. 32 (2015) 3526-40.

68. G.M. Dubowchik, R.A. Firestone, L. Padilla, D. Willner, S.J. Hofstead, K. Mosure, J.O. Knipe, S.J. Lasch, P.A. Trail, Cathepsin B-labile dipeptide linkers for lysosomal release of doxorubicin from internalizing immunoconjugates: model studies of enzymatic drug release and antigen-specific in vitro anticancer activity,

Bioconjug. Chem. 13 (2002) 855-69.

초 록

항체-약물 접합체에 사용할 항체 선별은 전통적으로 표적 세포에 대한 내재화에 의존해 왔으나 항체-약물 접합체의 효능 또한 수용체-항체-약물 접합체의 재활용, 엔도좀-리소좀 경로, 링커/항체 단백질분해에 의존한다. 우리는 이 논문에서 관심있는 항원 및 세포 독성 약물에 접합된 합텐에 동시에 결합하는 이중 특이성 single-chain variable fragment (scFv)-kappa constant region (Cκ)-scFv 융합 단백질로 구성된 새로운 항체-약물 접합체 개발 플랫폼을 설명한다. 코티닌은 비독성과 생물학적 시스템에 관여하지 않기 때문에 이상적인 합텐으로 선택하였다. 이 연구에서 우리는 이중 특이성 항 mPDGFRβ/코티닌 scFv-Cκ-scFv 융합 단백질과 코티닌-듀오카마이신을 준비하고, 이는 항체-약물 접합체 유사 복합체를 형성하고 mPDGFRβ 발현 세포에 독성을 유도할 수 있음을 관찰하였다. 다수의 항 mPDGFRβ 항체 후보 물질들을 이중 특이성 scFv-Cκ-scFv 융합 단백질 포맷으로 제조하고 코티닌-결합 세포 독성 약물을 전달하는 능력을 시험함으로써 항체-약물 접합체 제조에서 항체 선택을 위한 개선된 접근법을 제공한다.

주요어 : 항체-약물 접합체, 이중항체, 코티닌, 듀오카마이신

학번 : 2015-22055